European Journal of Medicinal Chemistry 243 (2022) 114730

Contents lists available at ScienceDirect

European Journal of Medicinal Chemistry

journal homepage: www.elsevier.com/locate/ejmech

Research paper

Enantioselective synthesis of 4-amino-3,4-dihydrocoumarins and their non-cyclic hydroxyester precursors: Biological evaluation for the treatment of glioblastoma multiforme

Lorenzo G. Borrego [a], Rocío Recio [a,*], Nazaret Moreno [a], Ahmed Chelouan [a], Eleuterio Álvarez [b], Antonio Sánchez-Coronilla [c], Carlos Caro [d], John R. Pearson [d], Maria Luisa García-Martín [d,e], Noureddine Khiar [b,**], Inmaculada Fernández [a,***]

[a] Departamento de Química Orgánica y Farmacéutica, Facultad de Farmacia, Universidad de Sevilla, C/ Profesor García González, 2, 41012, Sevilla, Spain
[b] Instituto de Investigaciones Químicas, CSIC-Universidad de Sevilla, Avda. Américo Vespucio, 49, 41092, Sevilla, Spain
[c] Departamento de Química Física, Facultad de Farmacia, Universidad de Sevilla, C/ Profesor García González, 2, 41012, Sevilla, Spain
[d] Instituto de Investigación Biomédica de Málaga y Plataforma en Nanomedicina (IBIMA Plataforma BIONAND), C/ Severo Ochoa, 35, 29590, Málaga, Spain
[e] Biomedical Research Networking Center in Bioengineering, Biomaterials & Nanomedicine (CIBER-BBN), Spain

ARTICLE INFO

Keywords:
Enantiopure 4-amino-3,4-dihydrocoumarins
N-sulfinylarylimines
Glioblastoma multiforme
β-hydroxyesters

ABSTRACT

The stereoselective addition of ethyl acetate enolate to the C=N bond of *N-tert*-butylsulfinylimines has been investigated in depth. A significant effect of the LHMDS amount and the *N*-sulfinylimine nature on the stereoselectivity of the process was observed. Conditions were found where sulfinylimines of differently substituted salicylaldehydes derivatives, ethyl acetate, and LHMDS afforded the corresponding addition products as a single diastereomer in good yields. The developed protocol was successfully applied to the first stereoselective synthesis of differently substituted 4-amino-3,4-dihydrocoumarin derivatives. Computational models confirmed the prominent role of the *ortho* aryl substituent in the stereoselectivity of the process. A significant and selective cytotoxic activity against Glioblastoma Multiforme (GBM) cancer line has been determined for the noncyclic hydroxy ester derivative.

1. Introduction

Synthetic and natural coumarins have received great interest due to their interesting biological activities [1]. Particularly attractive are 3, 4-dihydrocoumarins, as they hold a wide range of pharmacological activities including antimicrobial [2], estrogenic [3], antioxidant [4], antitumor [4a], immunomodulatory [4b], antihypertensive [1], antiplatelet [5], or anti-inflammatory [6] (Fig. 1). Given the significance of these chiral molecules, great effort has been devoted to their synthesis in an enantiopure form [7]. However, in the case of 3- and 4-amino-3, 4-dihydrocoumarins, which can be considered as α or β-amino acid derivatives, respectively, only a few approximations have been developed for the former [8], and to our knowledge, no asymmetric approximation has yet been developed for the preparation of the latter in enantiopure form. This is surprising as this motif is present, among others, in the general structure of the family of inhibitors of platelet aggregation **1** (Fig. 1). The interest of these derivatives lies in their activity as inhibitors of the integrin $\alpha_v\beta_3$ [9], a transmembrane adhesion glycoprotein that, in addition to being involved in platelet aggregation, participates in other physiopathological processes such as inflammation and angiogenesis [10]. Note that the active product is the hydroxy acid that results from the hydrolysis of the coumarin derivative. Therefore, the non-cyclic hydroxy esters of analogous structure could also be of interest as they can act as prodrugs in a similar way.

In addition, in recent years, coumarin and its derivatives have gained attention since they have demonstrated antitumor activity [11] by promoting many different cellular mechanisms, such as cell cycle arrest, kinase inhibition, or antimitotic activity [12]. Based on these premises and as part of our ongoing interest in the enantioselective synthesis of biologically relevant chiral amines [13], here we report an efficient and

* Corresponding author.
** Corresponding author.
*** Corresponding author.
E-mail address: rrecioj@us.es (R. Recio).

https://doi.org/10.1016/j.ejmech.2022.114730
Received 17 June 2022; Received in revised form 24 August 2022; Accepted 26 August 2022
Available online 1 September 2022

straightforward method for the stereoselective synthesis of 4-amino-3,4-dihydrocoumarin derivatives from low-cost raw materials and their hydroxy aminoesters precursors. An exhaustive *in vitro* screening has been conducted in order to determine their cytotoxicity in cancer and noncancer cell lines. The preliminary results on their selective cytotoxic activity against the Glioblastoma Multiforme (GBM) cancer line and an *in vivo* test with an orthotopic model of GBM after intratumoral administration are presented below.

2. Results and discussion

2.1. Diastereoselective synthesis of 4-amino-3,4-dihydrocoumarins and their noncyclic hydroxy ester analogues

A retrosynthetic scheme of 4-amino-3,4-dihydrocoumarins shows that they could be easily prepared using *tert*-butylsulfinylimines as a starting chiral substrate (Fig. 2). Indeed, sulfinylimines have been shown to be the starting substrates of choice for the stereoselective synthesis of various structurally diverse chiral amines [14].

A variety of nucleophiles of different nature have been added in a stereoselective manner to the CN double bond of *tert*-butylsulfinylimines, with high chemical and stereochemical yields, owing to the stereodirecting effect of the *tert*-butylsulfinyl group. According to the data found in the literature, the diastereoselectivity of this type of additions is strongly influenced by the nature of the nucleophile and the solvent [15]. The pioneering work of Ellman and Tang demonstrated that the addition of enolate to *N*-*tert*-butylsulfinylimines was a very effective methodology for the asymmetric synthesis of β-aminoacids [16]. No difference in the stereochemical outcome was observed in the addition of lithium, sodium, and titanium enolates, generated by LDA, NaHMDS, and $ClTi(OiPr)_3$, respectively (Fig. 3). However, the diastereoselectivity was only moderate in the case of the lithium and sodium enolates, while titanium enolates gave the highest chemical yields and diastereoselectivities. Additionally, these results were improved by increasing the amount of the otherwise highly toxic $ClTi(OiPr)_3$ (from 100 mol% to 200 mol%), providing the addition products in better yields (70–94%) and enhanced diastereoselectivities (90–98% de).

With the goal of developing the first approximation to enantiopure 4-amino-3,4-dihydrocoumarins, we decided to study the stereoselective addition of ethyl acetate lithium enolate to the corresponding *ortho* hydroxilated *N*-sulfinylarylimine (R = *o*-hydroxyphenyl, Fig. 3). Therefore, we focused on optimizing the reaction conditions to ensure a totally stereoselective process, using *N*-sulfinylimine **7a-(R_S)**, derived from salicylaldehyde, as substrate and LHMDS as base. Interestingly, it was found that it was not necessary to pregenerate the lithium enolate of ethyl acetate, which could be generated *in situ*, greatly simplifying the experimental conditions. Thus, by simply adding the base to a solution of sulfinylimine **7a-e** and ethyl acetate in THF at −78 °C afforded the corresponding sulfinamides **8a-e**. The stereoselectivity was strongly dependent on the amount of the base and ethyl acetate used. No reaction was observed when an equivalent amount of reagents (imine, ester, and base) were used (Entry 1, Table 1), and it proceeded without stereoselectivity when 100 mol% of ethyl acetate and an excess of base were used (entry 3, Table 1). The reaction took place in a totally stereoselective manner when the amount of base was increased to 200 mol% but with a moderate 50% yield (entry 2, Table 1). To our delight, when the amount of both ethyl acetate and LHMDS were increased, the nucleophilic addition was completely stereoselective, yielding quantitatively **8a-(R_S,S_C)** as a single diastereoisomer (entry 4, Table 1). In order to determine the generality of the process, the enolate ester was added to other sulfinylimines under different conditions, Table 1.

The analysis of the data collected in Table 1 allows the drawing of the following conclusions. First, the sulfinylimine/enolate ratio (**7-(R_S)**: AcOEt) determines the nature of the product obtained. Thus, with an excess of sulfinylimine **7b-(R_S)** (entry 5, Table 1), the 1,3-bis(sulfinamide) **9b-(R_S,R_C,S_C,S_C,R_S)** was obtained as the main product from a double addition process (Scheme 1).

Second, with equimolar amounts of both reagents, sulfinylimine and enolate, the monoaddition product is exclusively obtained, Scheme 1, (compare entries 5 *vs* entries 6 and 7, Table 1). Third, the stereochemical course of the reaction depends strongly not only on the amount of LHMDS used as the base, but also on the nature of the imine. The 2-naphtyl and *p*-methoxy substituted phenyl derivatives, **7b-(R_S)** and **7d-(R_S)**, always gave the (R_S,S_C) diasteromer as the major product with high but not complete stereoselectivity (74% and 82% de, respectively) (entries 7 and 12, Table 1). Finally, the stereoselectivity was only modest with the

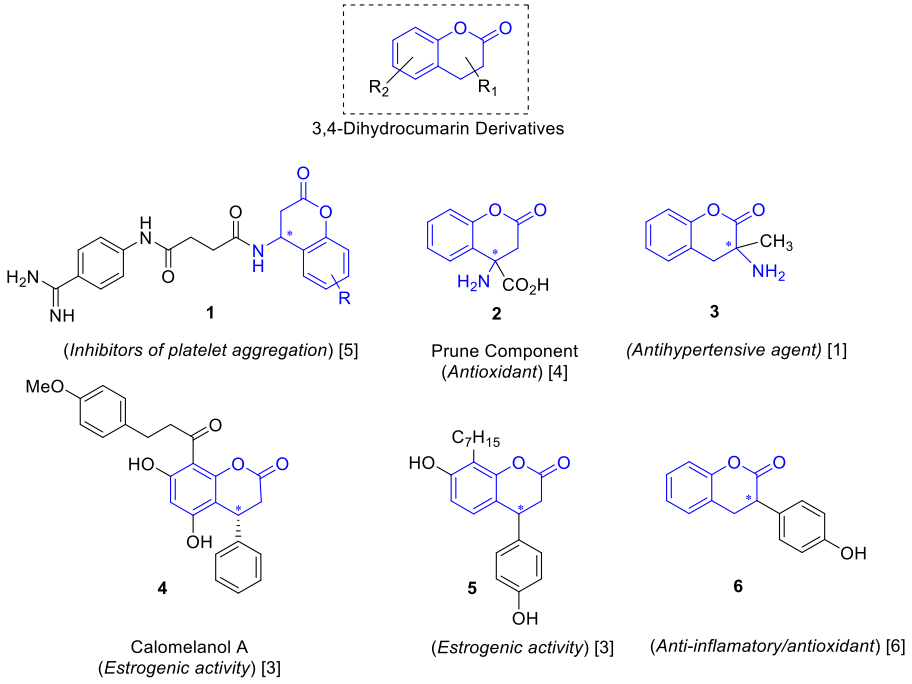

Fig. 1. Pharmacologycally remarkable dihydrocoumarins derivatives.

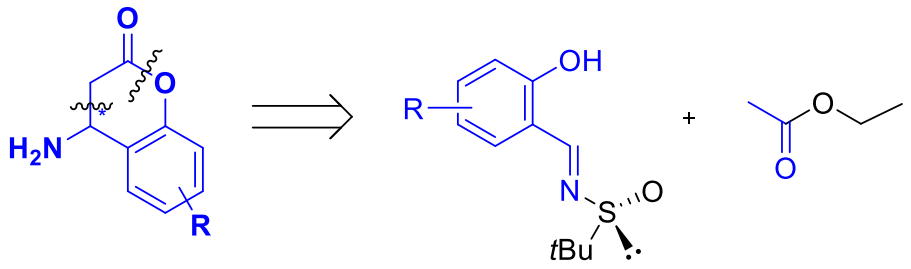

Fig. 2. Retrosynthetic scheme of the 4-amino-3,4-dihydrocoumarins.

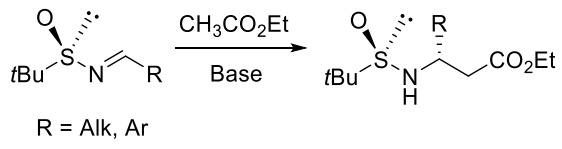

Base	R	Yield (%)	de(%)
LDA	Ph	76	66
NaHMDS	Ph	89	50
ClTi(O-*i*-Pr)$_3$ 100mol% /LDA	Ph	90	74
ClTi(O-*i*-Pr)$_3$ 200mol% /LDA	Alk, Ar	70-94	90-98

Fig. 3. Addition of different nucleophiles to *tert*-butylsulfinylimines.

Table 1
Stereoselective addition of ethyl acetate enolate to *N-tert*-butylsulfinylimines **7a-e-(R_S)**.

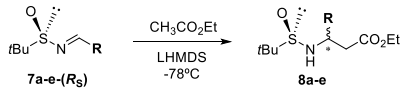

Entry	R_S (Sulfinylimine)	AcOEt (mol%)	LHMDS[a] (mol%)	Product[b]	Diast. Ratio[c] (R_S,S_C): (R_S,R_C)	de (%)	Yield (%)
1	2-(OH)C_6H_4 (**7a**)	100	100	**8a**	NR	–	0
2		100	200		100:0	100	50
3		100	500		52:48[d]	4	76
4		400	400		**100:0**	100	quant.
5	2-Napht (**7b**)	50	250	[e,f]	[e]	–	36
6		100	100	**8b**	70:30	40	61
7		100	500		**87:13**	74	quant.
8	2-(CH_3)C_6H_4 (**7c**)	100	100	**8c**	80:20	60	83
10		100	500		**100:0**	100	quant.
11	4-(CH_3O)C_6H_4 (**7d**)	100	100	**8d**	85:15	70	64
12		100	500		**91:9**	82	quant.
13	*i*Pr (**7e**)	100	100	**8e**	35:65	30	60
14		300	300		48:52	4	50
15		100	500		44:56	2	52

[a] The reaction was carried out by adding the base to a solution of the sulfinylimine and ethyl acetate in THF at −78 °C.
[b] The products are obtained after a reaction time of 1–2 h.
[c] The diasteromeric ratios are determined by NMR spectroscopy from the crudes.
[d] The product was partially degraded.
[e] LHMDS (500 mol%) is progressively added to a solution of the sulfinylimine (220 mol%) and ethyl acetate (100 mol%) in THF at −78 °C.
[f] 1,3-bis(sulfinamide) was obtained as the major compound.

alkyl sulfinylimine **7e-(R_S)** (entries 13–15, Table 1). In contrast, the *ortho*methyl substituted derivative **7c-(R_S)** yielded sulfinamide **8c-(R_S, S_C)** as a single diastereoisomer when the amount of base added was significantly increased (de: 100%, entry 10, Table 1). We propose that due to the strong basis conditions, the *ortho*methyl substituent must be deprotonated, as in the case of the hydroxyderivative **7a-(R_S)**.

The sense of the diastereoselection of the process as well as the absolute configurations of the obtained diasteroismers was determined by X-ray analysis and ^{1}H NMR spectroscopy. The main isomer **8d-(R_S,S_C)** obtained with the addition of ethyl acetate lithium enolate to *(R_S)-N-*(*p*-methoxybenzylidene)-2-methyl-2-propanesulfinamide **7d-(R_S)** (Table 1, entry 12) is crystalline and we could obtain an adequate crystal for the determination of its structure by X-ray (Fig. 4A). As can be seen, the absolute configuration of the newly created chiral centre is *S,* which allows us to confirm that the major isomer of the addition has the R_S,S_C configuration, and the minor isomer has the R_S,R_C absolute configuration.

The absolute configuration of the rest of nonhydoxylated sulfinamides was assigned based on their ^{1}H NMR spectra, taking as a reference the *p*-methoxy diastereomers **8d-(R_S,S_C)** and **8d-(R_S,R_C)**. The ^{1}H NMR signals corresponding to the ABX system of each pair of diastereoisomers have similar spectroscopic features with well-differentiated coupling patterns. The ABX system of the methylenic protons in the R_S,R_C diastereoisomers always present a very pronounced "non-equivalence" ($\Delta\nu$ = 77–110 Hz), while both methylene protons appear at almost the same chemical shift ($\Delta\nu$ around 20 Hz) in the R_S,S_C diastereoisomers.

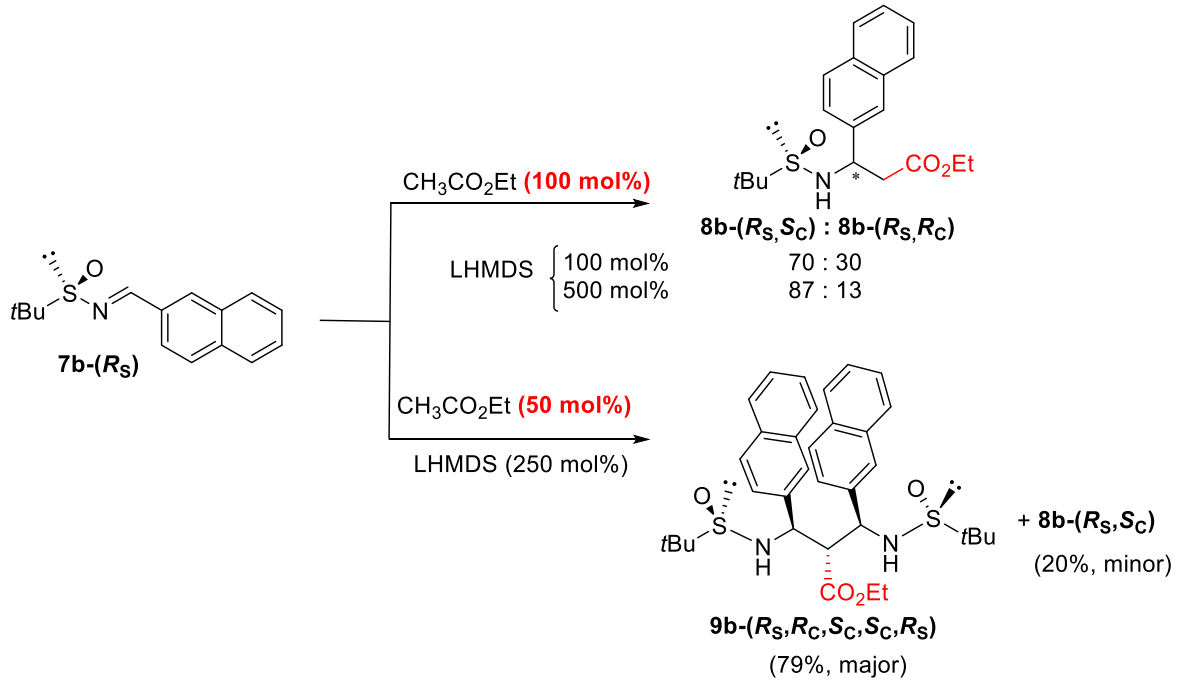

Scheme 1. Stereoselective synthesis of sulfinamide 8b-(RS,SC) and 1,3-bis-sulfinamide 9b-(RS, RC,SC,SC,RS).

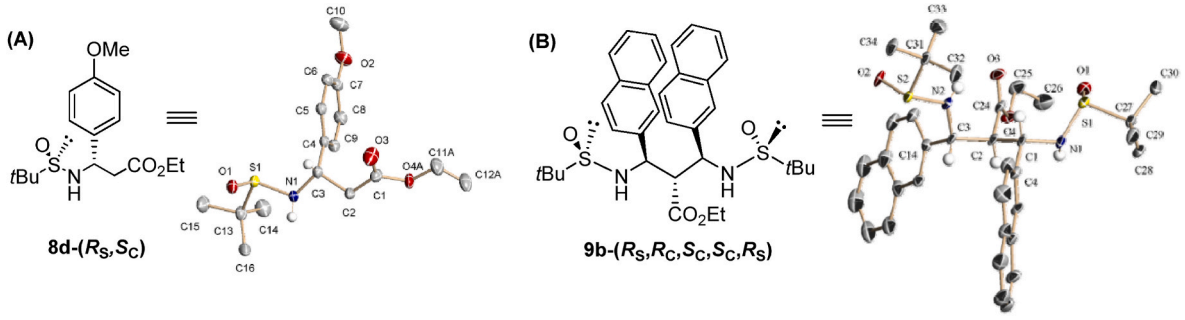

Fig. 4. (A) ORTEP drawing of the major sulfinamide **8d-(R_S,S_C).** (Thermal ellipsoids are shown at the 50% probability level, the hydrogen atoms are omitted for clarity). (B) ORTEP drawing of the 1,3-bis(sulfinamide) **9b-(R_S,R_C,S_C,S_C,R_S).**

In the case of 1,3-bis-sulfinamide, the diastereomer obtained **9b-(R_S, R_C,S_C,S_C,R_S)** lacks C_2 symmetry, according to the ^{1}H NMR spectrum, and the configuration was confirmed by X-ray analysis (Fig. 4). Therefore, unlike previously described additions of methyl sulfonyl carbanions [17], the stereochemical course of the second addition proceeds differently from the first addition step, due to the chiral carbon present in the intermediate enolate.

The peculiar stereochemical behavior of *N*-sulfinylimine **7a-(R_S)** must be attributed to the presence of the phenolic OH group. The complete stereoselectivity of the process prompted us to evaluate its substrate scope by adding lithium enolate from ethyl acetate to a series of *N*-sulfinylimines derived from differently substituted salicylaldehydes, under the optimized conditions (Entry 4, Table 1) and the results are collected in Table 2. The addition of both electron-deficient and electron-rich aromatic derivatives yielded the desired products in high chemical yields and with total diastereoselectivities, yielding the (R_S,S_C) diastereoisomer as the unique product.

Next, the transformation of these sulfinamides into the corresponding enantiopure 4-amino-3,4-dihydrocoumarins was studied. Attempts of lactonization of **8a-(R_S,S_C)** and **8f-m-(R_S,S_C)** under basic conditions, with LHMDS or $CaCO_3$, were unsuccessful. In the presence of *t*BuOK as a base, the desired products were obtained with very low yields along with cumarin derivatives as elimination products. Fortunately, in the presence of an excess of $BF_3{\cdot}OEt_2$ as Lewis acid and high dilution conditions, the desired lactones **10a-(R_S,S_C)**, **10f-g-(R_S,S_C)** and **10i-m-(R_S,S_C)** were obtained with high yields as the sole products (Scheme 2). The X-ray study of compound **10f-(R_S,S_C)** confirmed the configurational assignment of the new stereogenic center generated in the addition step.

Once again, in this process the *tert*-butylsulfinyl group can be considered not only as a chiral auxiliary but also as a protecting group of the amine function, which can be smoothly removed by treatment with HCl in dioxane. Therefore, the desulfinylation of **10a-(R_S,S_C)** and **10i-m-(R_S,S_C)** yields the hydrochlorides of the corresponding enantiopure 4-amino-3,4-dihydrocoumarins, **11a-(S_C)** and **11i-m-(S_C),** with a high yield as indicated in Scheme 3.

Similarly, desulfinylation of the non-cycled hydroxy esters, **8a-(R_S, S_C)** and **8a-(S_S,R_C), 8h-k-(R_S,S_C)** and **8m-(R_S,S_C)**, produces the corresponding β-aminoester hydrochlorides **12a-(S_C)** and **12a-(R_C), 12h-k (S_C)** and **12m-(S_C)** (Scheme 4).

2.1.1. *Justification of the observed stereoselectivity*

The singular and unusual total stereoselectivities observed in the addition of ester enolate to the imines of salicylaldehyde derivatives (**7a-(R_S), 7f-m-(R_S)**) are indicative of the primordial role of the phenolic

Table 2
Stereoselective addition of ethyl acetate enolate to *N-tert*-butylsulfinylimines of substituted salicylaldehydes **7a-(R_S)**, **7a-(S_S)** and **7f-m-(R_S)**.[a]

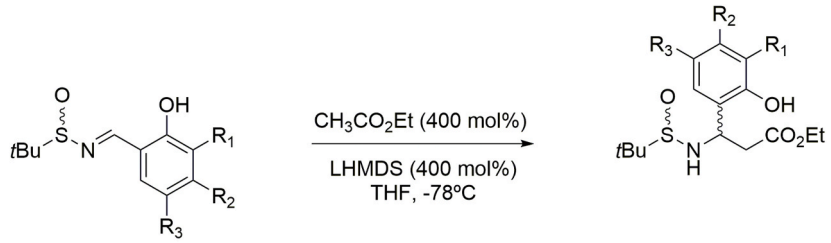

7a-(R_S), 7a-(S_S), 16f-m-(R_S) → **8a-(R_S,S_C), 8a-(S_S,R_C), 8f-m-(R_S,S_C)** 100% de

Entry	Sulfinylimine	R^1	R^2	R^3	Sulfinamide[b]	Yield (%)[c]
1	**7a-(R_S)**	H	H	H	**8a-(R_S,S_C)**	quant.
2	**7a-(S_S)**	H	H	H	**8a-(S_S,R_C)**	quant.
3	**7f-(R_S)**	Me	H	H	**8f-(R_S,S_C)**	75
4	**7g-(R_S)**	H	H	Me	**8g-(R_S,S_C)**	90
5	**7h-(R_S)**	H	OMe	H	**8h-(R_S,S_C)**	63
6	**7i-(R_S)**	H	H	OMe	**8i-(R_S,S_C)**	58
7	**7j-(R_S)**	OMe	H	Br	**8j-(R_S,S_C)**	quant.
8	**7k-(R_S)**	H	H	Br	**8k-(R_S,S_C)**	91
9	**7l-(R_S)**	H	NEt_2	H	**8l-(R_S,S_C)**	83
10	**7m-(R_S)**	H	H	NO_2	**8m-(R_S,S_C)**	92

[a] The reaction was carried out by adding LHMDS to a solution of the sulfinylimine and ethyl acetate in THF at −78 °C.
[b] The products are obtained after a reaction time of 1–2 h.
[c] Isolated yields.

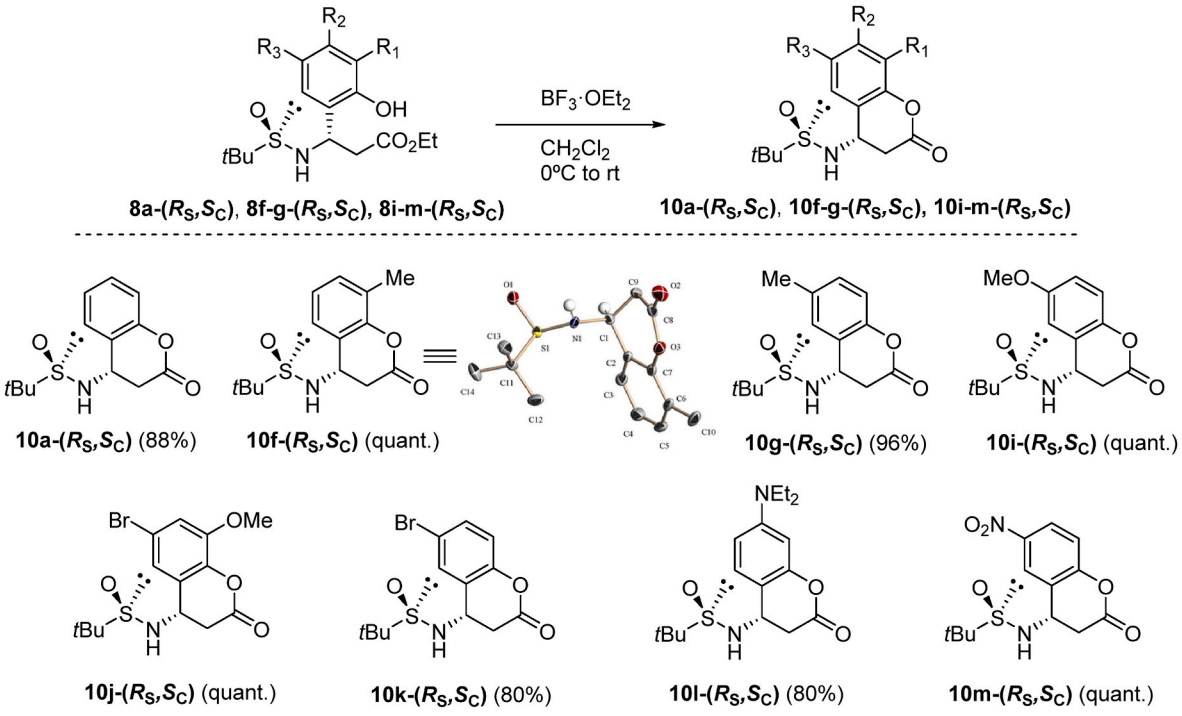

Scheme 2. Stereoselective synthesis of 4-tert-butylsulfinamide-3,4-dihydrocoumarins 10a-(RS,SC), 10f-g-(RS,SC) and 10i-m-(RS,SC).

hydroxyl group in the transition state of the nucleophilic addition. It can be assumed that the phenoxide anion formed under the basic medium is coordinated to the lithium cation of LHMDS, which is also coordinated to the enolate and the sulfinylimine in a Zimmerman-Traxler-type six-membered transition state. In this transition state, the *re* face of the imine is shielded by the *tert*-butyl group (Model A2, Fig. 5), so that the transfer of chirality from the *tert*-butylsulfinyl group takes place more effectively than in the traditionally proposed coordinated model A1, Fig. 5.

A similar situation could be proposed in the case of the *ortho* tolylderivative **7c-(R_S)**, which, being deprotonated in the presence of an excess of base, allows for a coordination (CH_2^- … Li^+) similar to that represented in model A2 through the benzylic carbon.

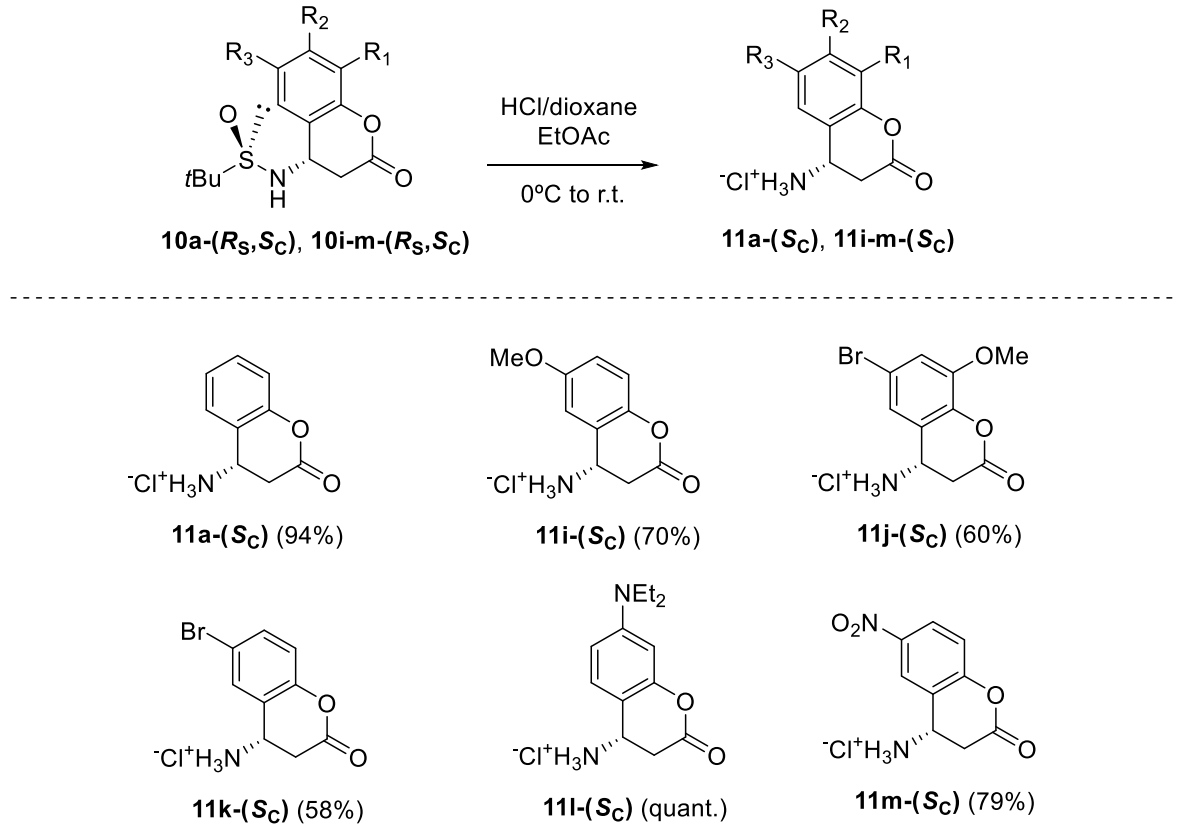

Scheme 3. Desulfinylation of 4-tert-butylsulfinamide-3,4-dihydrocoumarins 10a-(RS,SC) and 10i-m-(RS,SC).

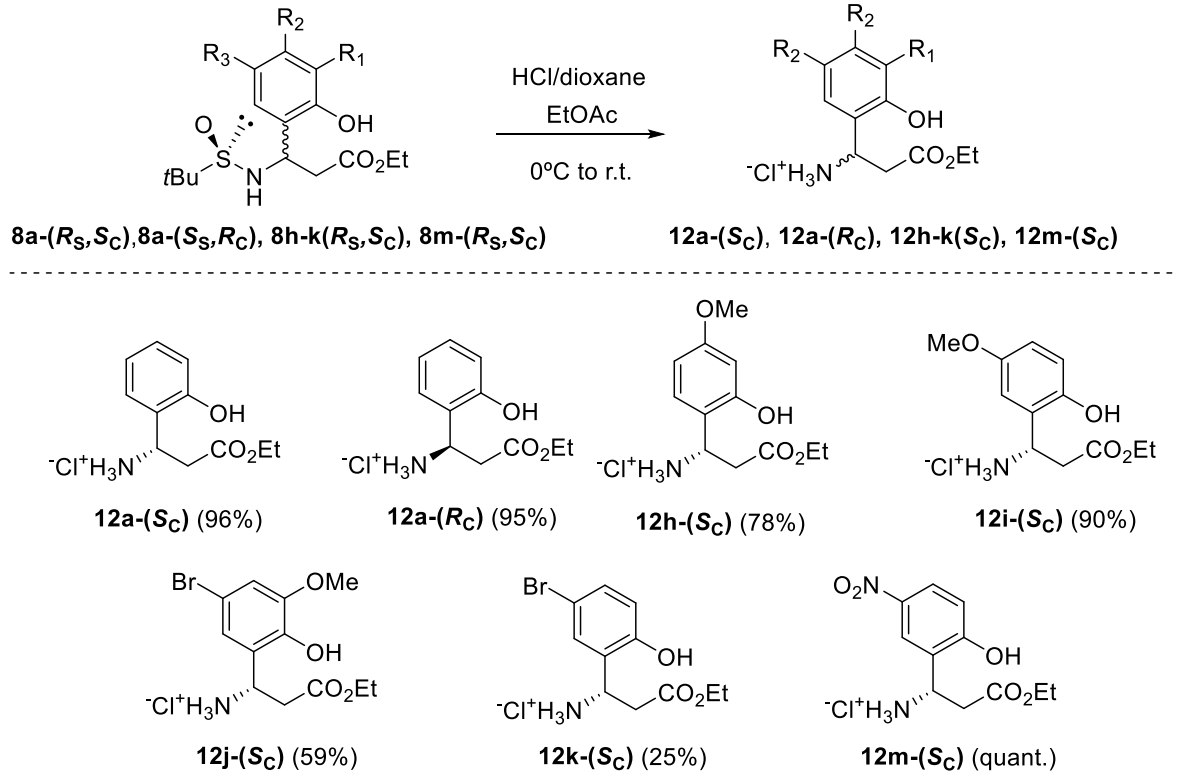

Scheme 4. Synthesis of noncyclic β-aminoester hydrochlorides 12a-(SC), 12a-(RC), 12h-k(SC) and 12m-(SC) by desulfinylation.

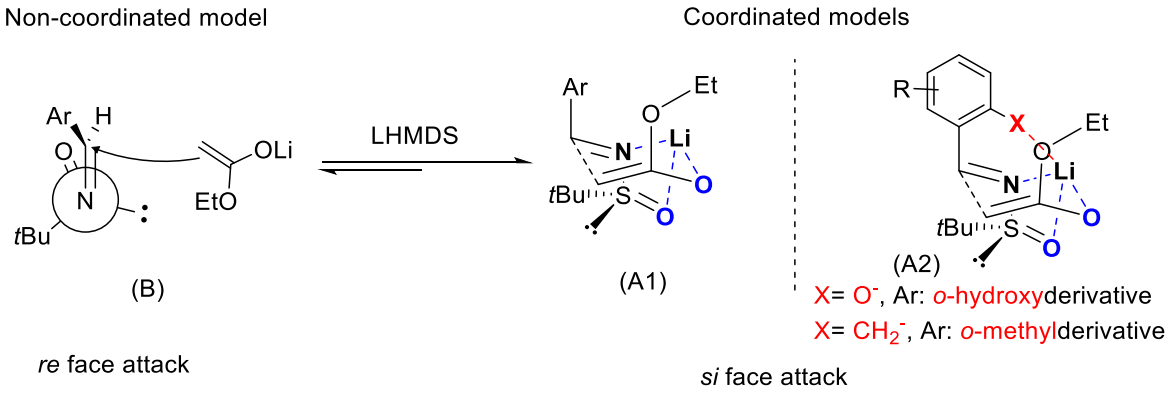

Fig. 5. Explanative model for the observed stereoselectivity.

2.2. Computational calculations

DFT calculations have been performed to understand the stability of the A1 and A2 transition states. Structures **7n-(R_S)** (X = H, Fig. 5) and **7a-(R_S)** (X = O^-, Fig. 5) were selected as reference for studying the coordinated transition states A1 and A2, respectively. The main difference in those structures is the presence of an *ortho* hydroxyl group in **7a-(R_S)**. The optimized geometries of both transition states are shown in Fig. 6. Energetically, it is found that model A2 is c.a. 2 kcal/mol more stable than model A1. With respect to the energetic values, it is understandable that the presence of the oxygen atom from the hydroxyl group may play a relevant role in stabilizing the transition state, leading to the total stereoselectivity of the process. A reasonable explanation for the stability of both A1 and A2 coordinated models is found by applying the Quantum Theory of Atoms in Molecules (QTAIM) to its optimized geometries (Fig. 6) [18]. The theory is based on the topological analysis of the density. According to this theory, for both transition states it is found a bond critical point (BCP) along a bond path between the carbon of

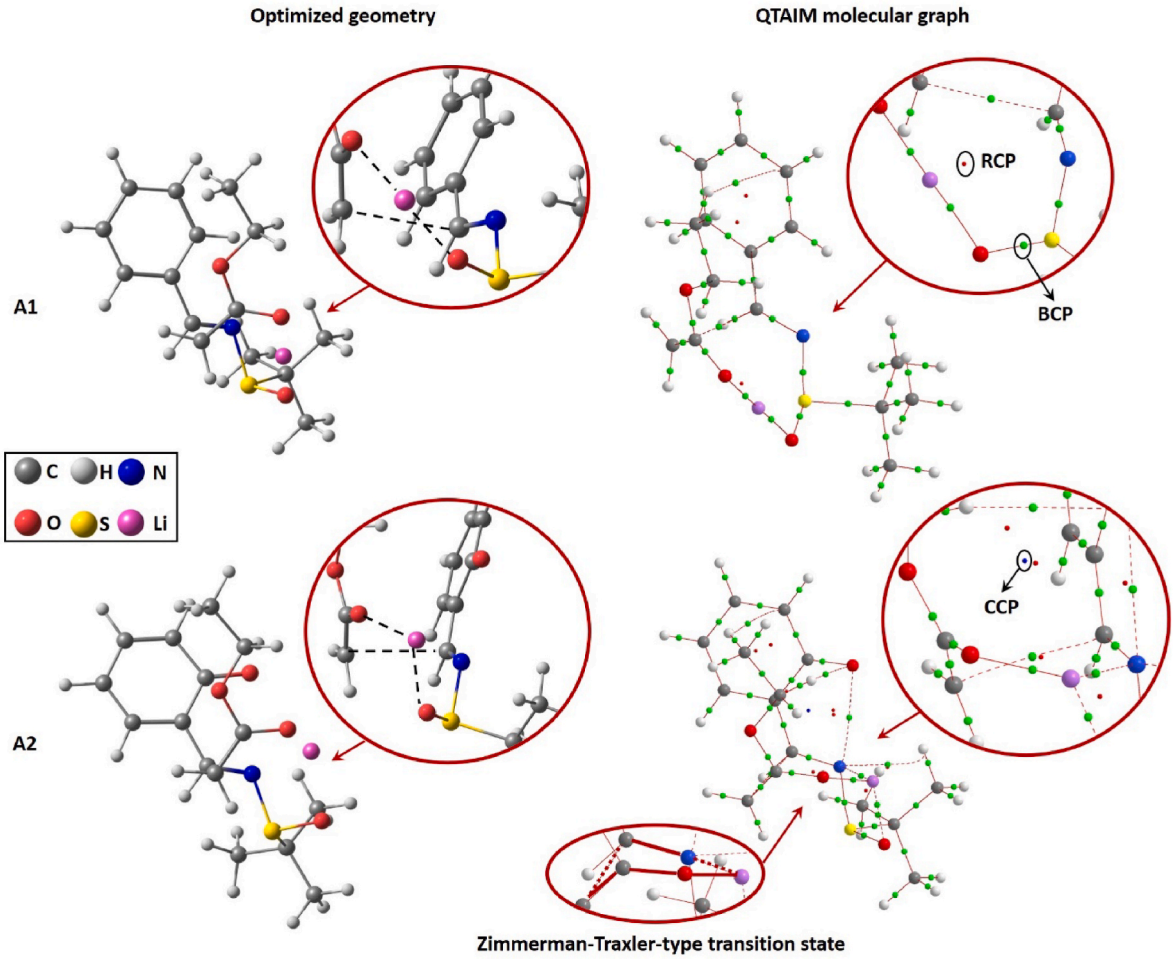

Fig. 6. Optimized geometries and molecular graphs for the model A1 and A2 transition states. In the QTAIM molecular graph the bond paths are in red lines, BCP, RCP and CCP in green, red and blue spheres, respectively.

ethyl acetate and the carbon atom from the CN bond of the sulfinylimine group (Fig. 6). For this BCP in both models, the values of electron density (ρ) and its Laplacian ($\nabla^2\rho$) are similar, 0.018a.u. and 0.044a.u., respectively. Interestingly, for model A2 the presence of the oxygen atom of the hydroxyl group generates a classic hydrogen bond O–H BCP with the hydrogen atom from the ethyl acetate (ρ = 0.004a.u.,$\nabla^2\rho$ = 0.015a.u.) and a O–N BCP between the oxygen atom (from the hydroxyl) and the N atom from the sulfinylimine group (ρ = 0.012a.u.,$\nabla^2\rho$ = 0.041a.u.). Low ρ and $\nabla^2\rho > 0$ values are typical of closed-shell interactions such as hydrogen bond, van der Waals, or ionic that stabilize the system [16]. Also, the molecular graph in Fig. 6 shows the presence of ring critical points (red-points in QTAIM analysis in Fig. 6). A critical ring point (RCP) is found in the interior of the bond path that forms a ring and stabilizes the system [18]. Model A1 presents three RCP, whereas the presence of the hydroxyl atom in Model A2 leads to new rearrangement of bond paths with the consequence appearance of new RCPs (Fig. 6). The new ring rearrangement of bond paths in model A2 are connected enclosing interstitial spaces arising one stabilizing cage critical point (CCP, in Fig. 6) that explains the highest stability of model A2 as compared to A1. Finally, it is worth pointing out that the disposition of the bond paths in model A2 obtained by applying QTAIM resembles the preferred Zimmerman-Traxler-type transition state (Fig. 6).

These results can be extrapolated to the rest of molecules with the presence of the *ortho* oxygen atom from hydroxyl group explaining its stereoselectivity. Furthermore, both model A1 and A2 transition states were found to be around 7 and 9 kcal/mol, respectively, more stable than the isopropyl derivative transition state (Fig. 7), which reveals the stabilizing role of phenyl ring in the process.

2.3. Biological activity

2.3.1. In vitro experiments

The antitumoral activity of the cyclic coumarins and their acyclic analogues was next investigated. To this we first performed a screening analysis by MTT using a plethora of different cell lines (non-cancer cells: N13/mouse microglial cell, BAEC/bovine aortic endothelial cells, and cancer cells: C6/rat glioblastoma multiforme cell, F98/rat glioblastoma multiforme cell, 4T1/mouse mammary cell, MCF7/human mammary cell, HeLa/human cervix cell) to compare the cytotoxic activity of the hydroxy-ester **12a-(S_C)** and the corresponding lactone derivative **11a-(S_C)** (Table 3 and Figs. S1–S2, see SI). The results revealed that both compounds had anticancer activity against GBM cells (mainly F98), while cyclic coumarin **11a-(S_C)** also showed toxicity in non-cancer cells. Hence, the hydroxy ester derivative **12a-(S_C)** was selected for further experiments. The hydroxy esters, **12a-(S_C)**, its enantiomer **12a-(R_C)**, **12h-k-(S_C)**, and **12m-(S_C)**, were evaluated using F98 as the cancer cell line and microglial N13 as the control, to determine the influence of chirality and chemical substitution of the aromatic ring on anticancer activity [19]. F98 was selected based on the screening results, as **12a-(S_C)** compound showed a higher antitumor activity, along with high selectivity for this cell line. The results demonstrated that the anticancer activity of these derivatives strongly depends on the chirality and chemical substitution of the aromatic rings (Table 3 and Figs. S3–S12, see SI), with **12a-(S_C)** again the one with the highest selectivity.

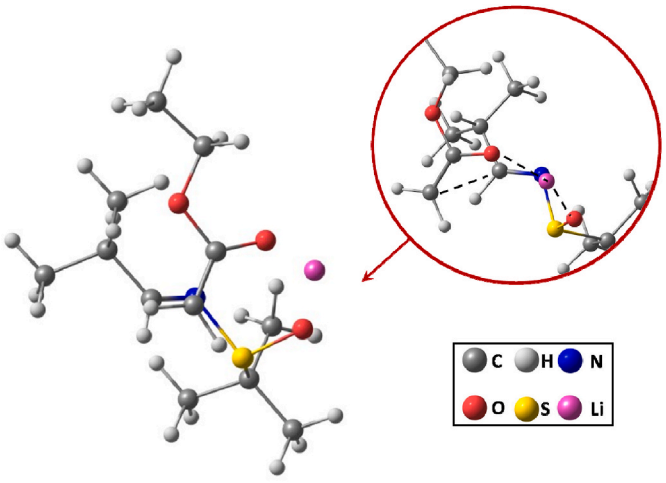

Fig. 7. Optimized geometry of isopropyl derivative transition state.

Consequently, **12a-(S_C)** was selected for further *in vitro* and *in vivo* experiments. To confirm the selectivity of **12a-(S_C)** for tumor cells, we performed assays on co-cultures of F98 and N13 cells. The two types have different morphologies and can be easily distinguished, with N13 cells being rounded and F98 cells having a much more elongated shape. However, as treatment could affect cell morphology, we also prelabeled N13 cells with the CM-Dil, a nontoxic compound that stably marks cellular membranes with red fluorescence [20]. Using Harmony software, we developed an automatic segmentation method that could distinguish between the two cell types with a high degree of confidence (Fig. S13, see SI). After exposure to **12a-(S_C)**, a dose-dependent decrease in the number of elongated F98 cells was easily detectable, while the number of spherical N13 cells remained approximately the same (Fig. 8A–C). Automatic quantification of the two cell types confirmed that this dose-dependent response to **12a-(S_C)** treatment was statistically significant ($p < 0.05$) (Fig. 8D), with a large increase in N13 cells after 24 h of treatment (Fig. 8E).

In order to determine the mechanism of cell death pathway, the cell cycle of both N13 and F98 after exposure to 100 μg/mL of **12a-(S_C)** for 24 h was assessed by flow cytometry. Cellular DNA content can be used to estimate the frequency of cell cycle phases ($G_{0/1}$ vs. S vs. G_2M). Apoptotic cells (sub G_0/G_1 region) are characterized by fractional DNA content and, therefore, can be easily identified by this technique [21] Analysis of the sub G_0/G_1 fraction revealed no features of apoptosis in N13 cells, with no differences between treated and untreated cells (Fig. S14a, see SI), whereas in F98 cells, a statistically significant increase of 42% in sub G_0/G_1 fraction was observed in treated cells compared to controls (Fig. S14b, see SI). These results indicate that F98 cells exposed to **12a-(S_C)** followed an apoptotic cell death pathway.

2.3.2. In vivo experiments

To evaluate the potential effects of **12a-(S_C)** on the healthy brain parenchyma, a local administration inside the caudate nucleus of non-tumor-bearing rats was carried out, and the possible effects were assessed by *in vivo* Magnetic Resonance Imaging (MRI). Furthermore, the survival rate of the animals was also monitored. In addition, PBS was also injected into the same brain region as control. Magnetic resonance imaging did not detect evidence of brain injury, even 30 days after local administration of both PBS and **12a-(S_C)** (Fig. 9A). Furthermore, the animals did not show any external evidence of pain or suffering, and the survival rate after 30 days was 100% in all cases (Fig. 9B).

Once the safety of normal brain tissue after local exposure to **12a-(S_C)** was confirmed, its therapeutic potential was evaluated *in vivo* in F98 tumor-bearing rats. After tumor implantation, tumor volume was calculated at different time points (3,5,8,10,12, and 15 days) using T_2-weighted images. When tumor volume reached around 325 mm^3 (day 10), PBS alone or **12a-(S_C)** in PBS were intratumorally administered. No noticeable effect on the tumor was observed for rats administered with PBS, whereas two days after the intratumoral administration of **12a-(S_C)**, tumors exhibited a pronounced darkening inside, which can be attributed to necrotic/apoptotic processes (Fig. 10A). Furthermore, the therapeutic effect was evaluated by measuring the volume of the tumor over time. On day 10 after implantation, the average tumor volume was 325 mm^3 for all animals. At this time, the animals were separated into two groups and injected with PBS or **12a-(S_C)**, as previously described. Two days later, the average tumor size of the PBS group increased to 845 mm^3, while tumors of the **12a-(S_C)** group maintained

Table 3
Summary of MTT assays for **12a-(S_C)**, **12a-(R_C)**, **12h-k-(S_C)** and **12m-(S_C)**. Grading of cytotoxicity according to ISO 10993-5.

Entry	Compound	Highest Concentration		Cytotoxicity on N13	IC50 (mM)	Grading of cytotoxicity N13	Cytotoxicity on F98	IC50 (mM)	Grading of cytotoxicity F98
		μg/ml	μM						
1	**12a-(S_C)**	100	0.40	0 ± 3%	–	None	60 ± 2%	0.14	Moderate
2	**12a-(R_C)**	100	0.40	40 ± 5%	0.45	Mild	35 ± 10%	0.78	Mild
3	**11a-(S_C)**	100	0.50	15 ± 5%	1.57	Slight	55 ± 2%	0.48	Moderate
6	**12h-(S_C)**	100	0.36	55 ± 2%	0.34	Moderate	45 ± 5%	0.47	Moderate
7	**12i-(S_C)**	100	0.36	70 ± 2%	0.04	Moderate	5 ± 3%	–	Slight
8	**12j-(S_C)**	100	0.28	60 ± 2%	0.22	Moderate	60 ± 3%	0.17	Moderate
9	**12k-(S_C)**	100	0.31	40 ± 3%	0.5	Mild	60 ± 2%	0.21	Moderate
10	**12m-(S_C)**	100	0.34	30 ± 5%	0.66	Mild	20 ± 5%	1.14	Slight

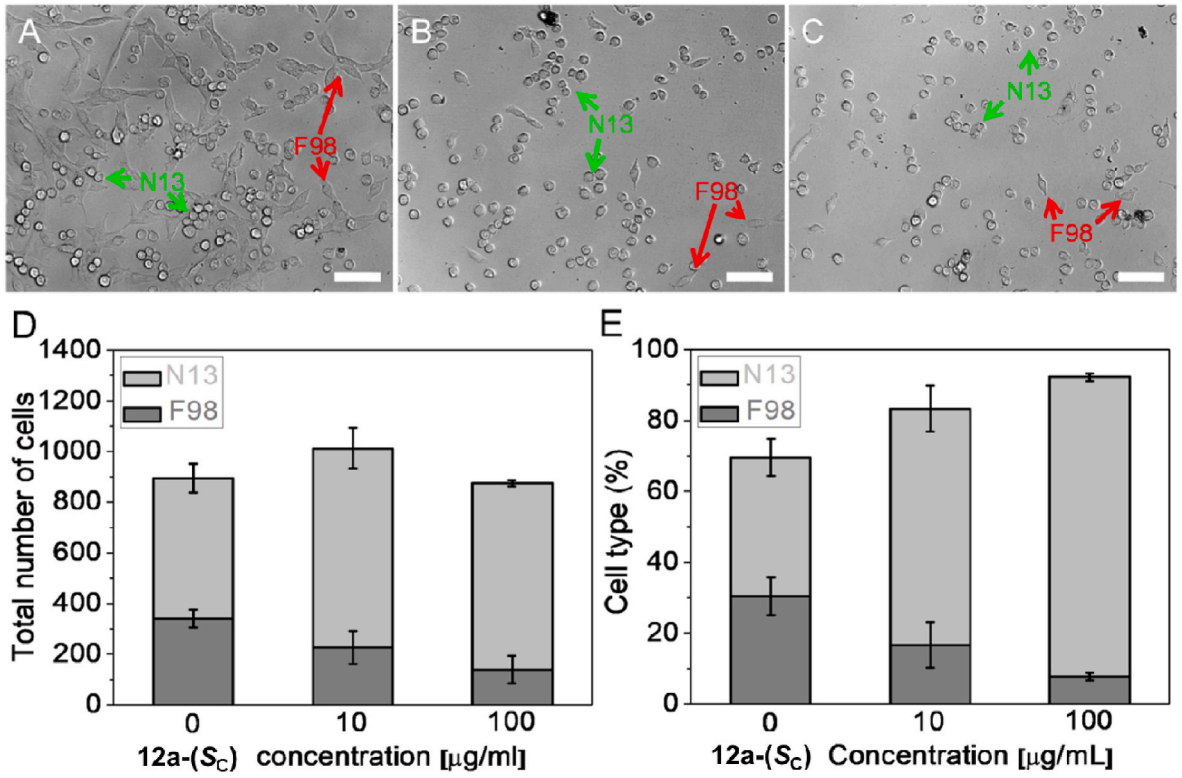

Fig. 8. Representative brightfield microscopy images of the co-culture of N13 and F98 cells exposed to different concentration of **12a-(S_C)**: (A) 0 μg/mL (B) 10 μg/mL (C) 100 μg/mL. Green arrows indicate N13 cells, whereas red arrows indicate F98 cells. Scale bar corresponds to 50 μm. Total number of cell (D) and cell percentage (E) of N13 and F98 cells after exposure to different concentrations of **12a-(S_C)**.

approximately the same volume (370 mm^3). Finally, five days after intratumoral administration, the animals in the PBS group could not survive tumor growth, while the animals in the **12a-(S_C)** group were still alive, with an average tumor size of 815 mm^3 (Fig. 10B). Furthermore, the survival rate analysis revealed that while all the animals in the PBS group died 13 days after tumor implantation, animals in the **12a-(S_C)** group survived an additional 3 days (Fig. 10C). In conclusion, intratumoral administration of **12a-(S_C)**, caused appreciable tumor tissue damage, as could be observed in the MR images, leading to a delay in tumor growth and an increase in overall survival of 3 days. Interestingly, these results are similar to those obtained after intratumoral delivery of bortezomib in a GBM model [22].

3. Conclusions

In summary, we have reported the first enantioselective synthesis of 4-amino-3,4-dihydrocoumarins. The method which has allowed us the synthesis of a wide range of enantiopure 4-amino-3,4-dihydrocoumarin derivatives and their noncyclic hydroxy ester analogues is based on the stereoselective addition of ethyl acetate lithium enolate to the corresponding *N-tert*-butylsulfinylimines. The main advantage of this methodology is double: *(i)* it is a simple four-step synthesis, from commercially available starting material and *(ii)* the key step of addition of ethyl acetate lithium enolate to the CN bond takes place in a completely stereoselective manner. The biological activity studies demonstrate that both chirality and chemical substitution of the aromatic ring in the ethyl hydroxy esters derivatives are key aspects for selective toxicity against cancer cells. This selectivity was tested and confirmed in co-culture of cancer and non-cancer cells. Furthermore, the selected non-cyclic derivative **12a-(S_C)** exhibited good performance for the treatment of GBM *in vivo*, after intratumoral administration, without affecting normal brain tissue. Therefore, the results presented here show the great potential of the hydroxy ester derivative **12a-(S_C)** as an antitumor agent and could open new avenues in the treatment of GBM.

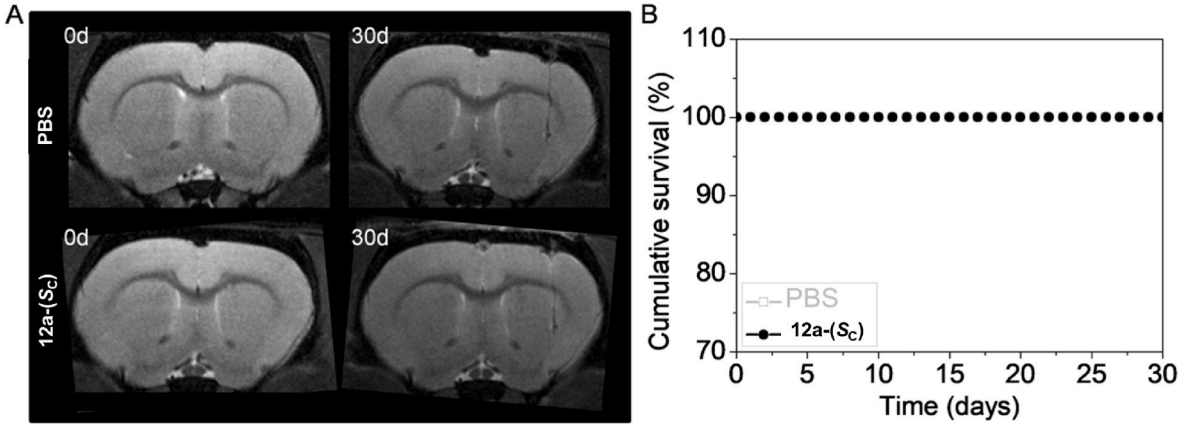

Fig. 9. (A) Representative MR images of rat brains before and 30 days after the administration of PBS (top) and **12a-(S_C)** (bottom) into the caudate nucleus. (B) Survival analysis by Kaplan-meier plot after the injection of PBS and **12a-(S_C)**.

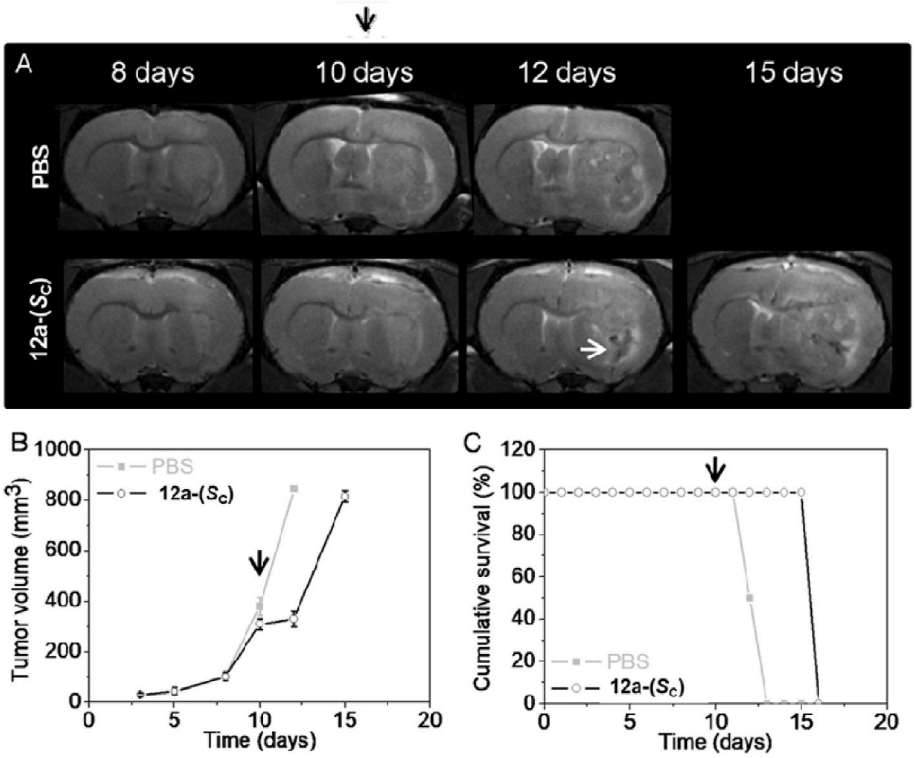

Fig. 10. (A) Representative MR images of brain tumor-bearing rats at different time points after the implantation. Rats were intratumorally injected with PBS or **12a-(S_C)**. White arrow indicates injected zone. (B) Tumor volume evaluation at different time points after the implantation. (C) Survival analysis by Kaplan-meier plot. In both cases, the black arrows indicate the administration point.

4. Experimental section

4.1. Synthesis

All reactions were run under an atmosphere of dry argon using oven-dried glassware and freshly distilled and dried solvents. THF, EtOAc, CH_2Cl_2, diethyl ether were dried using molecular sieves, and highest quality solvents were used. The chemicals were obtained from commercial sources and used without further purification. TLC was carried out on silica gel GF254 (Merck), and compounds were detected by charring with phosphomolybdic acid/EtOH. For flash chromatography, Merck 230–400 mesh silica gel was used. Chromatographic columns were eluted with a positive pressure of air, and the eluents are given as volume-to-volume ratios (v/v). NMR spectra were recorded with Bruker Avance 300 and 500 MHz spectrometers, using Me4Si as an internal reference. Chemical shifts are reported in ppm, and coupling constants are reported in Hz. High-resolution mass spectra (HRMS) were recorded in the Centro de Investigación, Tecnología e Innovación in the University of Seville with a Kratos MS-80RFA 241-MC apparatus. Optical rotations were determined with a Perkin–Elmer 341 polarimeter. Melting points were measured with a Stuart SMP3 apparatus in open-ended capillary tubes.

*4.1.1. **Synthesis of N-sulfinylimines:** general procedure [14d-f]*

To a solution of the corresponding aldehyde (100 mol%) and the (*R*)-*tert*-butanesulfinamide (110 mol%) in dry THF, at room temperature under argon atmosphere, $Ti(OEt)_4$ (110 mol%) was added. Once the starting material was consumed (24–48 h), the reaction mixture is

hydrolyzed with a saturated NaCl aqueous solution. The resulting suspension was filtered through a pad of Celite. The aqueous phase was extracted with CH_2Cl_2 (3 × 40 mL) and the combined organic phases were dried with anhydrous Na_2SO_4. The solvent was evaporated under reduced pressure and the reaction crude was purified by flash chromatography to obtain the desired compound.

(R_S)-N-(o-Hydroxybenzylidene)-2-methyl-2-propanesulfinamide, **7a-(R_S)** [23]. It was prepared following the general procedure from 2 g of (*R*)-*tert*-butanesulfinamide (16.5 mmol), 1.57 mL of salicylaldehyde (15 mmol) and 3.46 mL of $Ti(OEt)_4$ (16.5 mmol). After 24 h, the resulting residue was purified by flash chromatography (EtOAc:hexane, 1:5) to give 3 g of **7a-(R_S)** (13.3 mmol, 89% yield) as a white solid; mp 93–94 °C; $[\alpha]_D^{20}$ +61.4 (*c* 1, $CHCl_3$); ^{1}H NMR (500 MHz, $CDCl_3$): δ 11.03 (bs, 1H), 8.70 (s, 1H), 7.50–7.42 (m, 2H), 7.04–6.97 (m, 2H), 1.27 (s, 9H) ppm; ^{13}C NMR (125 MHz, $CDCl_3$): δ 165.8, 160.6, 135.1, 133.7, 120.2, 118.7, 117.7, 58.2, 22.6 ppm; HRMS (ESI) *m/z*: $[M + Na]^+$ Calcd for $C_{11}H_{15}O_2NNaS$ 248.0711; found 248.0716.

(S_S)–N-(o-Hydroxybenzylidene)-2-methyl-2-propanesulfinamide, **7a-(S_S)** [23]. It was prepared following the general procedure from 2 g of (*S*)-*tert*-butanesulfinamide (16.5 mmol), 1.57 mL of salicylaldehyde (15 mmol) and 3.46 mL of $Ti(OEt)_4$ (16.5 mmol). After 24 h, the resulting residue was purified by flash chromatography (EtOAc:hexane, 1:5) to give 2.77 g of **7a-(S_S)** (12.3 mmol, 82% yield) as a white solid eith similar spectroscopic characteristics than **7a-(R_S)**; mp 94 °C; $[\alpha]_D^{20}$ − 60.8 (*c* 1, $CHCl_3$); HRMS (ESI) *m/z*: $[M + Na]^+$ Calcd for $C_{11}H_{15}O_2NNaS$ 248.0711; found 248.0716.

(R_S)-N-[(2-Naphthyl)methylidene]-2-methyl-2-propanesulfinamide, **7b-(R_S)** [13a]. It was prepared following the general procedure from 5 g of (*R*)-*tert*-butanesulfinamide (41.3 mmol), 5.86 mL of 2-naphthaldehyde (37.5 mmol) and 8.66 mL of $Ti(OEt)_4$ (41.3 mmol). After 24 h, the resulting residue was purified by flash chromatography (EtOAc:hexane, 1:10) to give 9.18 g of **7b-(R_S)** (35.4 mmol, 95% yield) as a white solid; mp 112–113 °C; $[\alpha]_D^{20}$ − 173.7 (*c* 1, $CHCl_3$); ^{1}H NMR (500 MHz, $CDCl_3$): δ 8.76 (s, 1H), 8.21 (s, 1H), 8.04 (dd, *J* = 1.5 and 8.6 Hz, 1H), 7.96–7.94 (m, 1H), 7.91–7.87 (m, 2H), 7.61–7.54 (m, 2H), 1.30 (s, 9H) ppm; ^{13}C NMR (125 MHz, $CDCl_3$): δ 162.9, 135.6, 133.2, 132.6, 132.0, 129.3, 129.0, 128.4, 128.1, 127.1, 124.0, 58.0, 22.8 ppm. HRMS (ESI) *m/z*: $[M + Na]^+$ Calcd for $C_{15}H_{17}NOSNa$ 282.0918; found 282.0923.

(R_S)-N-(o-Methylbenzylidene)-2-methyl-2-propanesulfinamide, **7c-(R_S)** [24]. It was prepared following the general procedure from 5 g of (*R*)-*tert*-butanesulfinamide (41.3 mmol), 4.34 mL of 2-methylbenzaldehyde (37.5 mmol) and 8.66 mL of $Ti(OEt)_4$ (41.3 mmol). After 20 h, the resulting residue was purified by flash chromatography (EtOAc:hexane, 1:12) to give 7.64 g of **7c-(R_S)** (34.2 mmol, 91% yield) as a yellow liquid; $[\alpha]_D^{20}$ − 130.1 (*c* 1, $CHCl_3$); ^{1}H NMR (500 MHz, $CDCl_3$): δ 8.85 (s, 1H), 7.90 (dd, *J* = 0.7 and 7.7 Hz, 1H), 7.38 (td, *J* = 1.2 and 7.5 Hz, 1H), 7.30–7.24 (m, 2H), 2.60 (s, 3H), 1.27 (s, 9H) ppm; ^{13}C NMR (125 MHz, $CDCl_3$): δ 161.9, 139.6, 132.4, 132.1, 131.5, 129.7, 126.5, 57.7, 22.7, 20.1 ppm; HRMS (ESI) *m/z*: $[M + Na]^+$ Calcd for $C_{12}H_{17}ONNaS$ 246.0923; found 246.0918.

(R_S)-N-(p-Methoxybenzylidene)-2-methyl-2-propanesulfinamide, **7d-(R_S)** [24]. It was prepared following the general procedure from 2 g of (*R*)-*tert*-butanesulfinamide (16.5 mmol), 1.83 mL of 4-methoxylbenzaldehyde (15 mmol) and 3.46 mL of $Ti(OEt)_4$ (16.5 mmol). After 24 h, the resulting residue was purified by flash chromatography (EtOAc: hexane, 1:8) to give 2.90 g of **7d-(R_S)** (12.12 mmol, 81% yield) as a white solid; mp 95–97 °C; $[\alpha]_D^{20}$ − 59.8 (*c* 1, $CHCl_3$); ^{1}H NMR (500 MHz, $CDCl_3$): δ 8.51 (s, 1H), 7.81 (d, *J* = 11.5 Hz, 2H), 6.97 (d, *J* = 11.5 2H), 3.87 (s, 3H), 1.25 (s, 9H) ppm; ^{13}C NMR (125 MHz, $CDCl_3$): δ 163.2, 161.9, 131.4, 127.5, 114.5, 57.7, 55.6, 22.7 ppm; HRMS (ESI) *m/z*: $[M + Na]^+$ Calcd for $C_{12}H_{17}O_2NNaS$ 262.0865; found 262.0872.

(R_S)-N-(2-Methyl-1-propylidene)-2-methyl-2-propanesulfinamide, **7e-(R_S)** [13a]. It was prepared following the general procedure from 5 g of (*R*)-*tert*-butanesulfinamide (41.3 mmol), 5.59 mL of isopropylaldehyde (61.5 mmol) and 8.66 mL of $Ti(OEt)_4$ (41.3 mmol). After 24 h, the resulting residue was purified by flash chromatography (EtOAc:hexane, 1:20) to give 7.29 g of **7e-(R_S)** (41.5 mmol, quantitative yield) as a yellow liquid; $[\alpha]_D^{20}$ − 253.2 (*c* 1, $CHCl_3$); ^{1}H NMR (500 MHz, $CDCl_3$): δ 7.93 (d, *J* = 4.4 Hz, 1H), 2.70–2.61 (m, 1H), 1.19 (s, 9H), 1.12 (d, *J* = 2.4 Hz, 3H), 1.10 (t, *J* = 2.4 Hz, 3H) ppm; ^{13}C NMR (125 MHz, $CDCl_3$): δ 173.9, 56.7, 35.1, 22.5, 19.1 ppm; HRMS (ESI) *m/z*: $[M + H]^+$ Calcd for $C_8H_{18}ONS$ 176.1100; found 176.1104.

(R_S)-N-(2-Hydroxy-3-methylbenzylidene)-2-methyl-2-propanesulfinamide, **7f-(R_S)**. It was prepared following the general procedure from 2 g of (*R*)-*tert*-butanesulfinamide (16.5 mmol), 1.82 mL of 2-hydroxy-3-methylbenzaldehyde (15 mmol) and 3.46 mL of $Ti(OEt)_4$ (16.5 mmol). After 24 h, the resulting residue was purified by flash chromatography (EtOAc:hexane, 1:10) to give 3.39 g of **7f-(R_S)** (14.2 mmol, 94% yield) as a yellow solid; mp 51–53 °C $[\alpha]_D^{20}$ +100.7 (*c* 1, $CHCl_3$); ^{1}H NMR (500 MHz, $CDCl_3$): δ 11.26 (s, 1H), 8.69 (s, 1H), 7.33–7.31 (m, 2H), 6.90 (t, *J* = 7.6 Hz, 1H), 2.30 (s, 3H), 1.27 (s, 9H) ppm; ^{13}C NMR (125 MHz, $CDCl_3$): δ 165.8, 158.7, 135.9, 131.2, 126.6, 119.6, 117.8, 57.9, 22.4, 15.6 ppm; HRMS (ESI) *m/z*: $[M+Na]^+$ Calcd for $C_{12}H_{17}O_2NNaS$ 262.0866; found 262.0872.

(R_S)-N-(2-Hydroxy-5-methylbenzylidene)-2-methyl-2-propanesulfinamide, **7g-(R_S)**. It was prepared following the general procedure from 2 g of (*R*)-*tert*-butanesulfinamide (16.5 mmol), 2.04 g of 2-hydroxy-5-methylbenzaldehyde (15 mmol) and 3.46 mL of $Ti(OEt)_4$ (16.5 mmol). After 24 h, the resulting residue was purified by flash chromatography (EtOAc:hexane, 1:10) to give 2.98 g of **7g-(R_S)** (12.5 mmol, 83% yield) as a yellow solid; mp 127–129 °C $[\alpha]_D^{20}$ +21.2 (*c* 1, $CHCl_3$); ^{1}H NMR (500 MHz, $CDCl_3$): δ 10.83 (s, 1H), 8.66 (s, 1H), 7.25 (m, 2H), 6.93–6.91 (m, 1H), 2.32 (s, 3H), 1.26 (s, 9H) ppm; ^{13}C NMR (125 MHz, $CDCl_3$): δ 165.6, 158.3, 135.8, 133.4, 129.2, 118.1, 117.3, 57.9, 22.4, 20.4 ppm; HRMS (ESI) *m/z*: $[M+Na]^+$ Calcd for $C_{12}H_{17}O_2NNaS$ 262.0865; found 262.0872.

(R_S)-N-(2-Hydroxy-4-metoxybenzylidene)-2-methyl-2-propanesulfinamide, **7h-(R_S)** [25]. It was prepared following the general procedure from 2 g of (*R*)-*tert*-butanesulfinamide (16.5 mmol), 2.28 g of 2-hydroxy-4-metoxybenzaldehyde (15 mmol) and 3.46 mL of $Ti(OEt)_4$ (16.5 mmol). After 24 h, the resulting residue was purified by flash chromatography (EtOAc:hexane, 1:10) to give 2.42 g of **7h-(R_S)** (9.49 mmol, 63% yield) as a white solid; mp 131–133 °C $[\alpha]_D^{20}$ +90.4 (*c* 1, $CHCl_3$); ^{1}H NMR (500 MHz, $CDCl_3$): δ 11.32 (s, 1H), 8.60 (s, 1H), 7.36 (d, *J* = 8.6 Hz, 1H), 6.54 (dd, *J* = 2.4 and 8.6 Hz, 1H), 6.50 (d, *J* = 2.4 Hz, 1H), 3.85 (s, 3H), 1.25 (s, 9H) ppm; ^{13}C NMR (125 MHz, $CDCl_3$): δ 165.3, 164.3, 162.7, 134.9, 112.6, 107.9, 101.3, 57.7, 55.7, 22.4 ppm; HRMS (ESI) *m/z*: $[M + Na]^+$ Calcd for $C_{12}H_{17}O_3NNaS$ 278.0815; found 278.0821.

(R_S)-N-(2-Hydroxy-5-metoxybenzylidene)-2-methyl-2-propanesulfinamide, **7i-(R_S)**. It was prepared following the general procedure from 2 g of (*R*)-*tert*-butanesulfinamide (16.5 mmol), 1.87 mL of 2-hydroxy-5-metoxybenzaldehyde (15 mmol) and 3.46 mL of $Ti(OEt)_4$ (16.5 mmol). After 24 h, the resulting residue was purified by flash chromatography (EtOAc:hexane, 1:5) to give 3.33 g of **7i-(R_S)** (13.0 mmol, 87% yield) as a yellow solid; mp 123–126 °C $[\alpha]_D^{20}$ +20.9 (*c* 1, $CHCl_3$); ^{1}H NMR (500 MHz, $CDCl_3$): δ 10.62 (s, 1H), 8.65 (s, 1H), 7.06 (dd, *J* = 3.0 and 9.0 Hz, 1H), 6.96–6.95 (m, 2H), 3.80 (s, 3H), 1.26 (s, 9H) ppm; ^{13}C NMR (125 MHz, $CDCl_3$): δ 165.3, 154.7, 152.9, 122.6, 118.4, 118.0, 115.8, 58.0, 56.1, 22.4 ppm; HRMS (ESI) *m/z*: $[M + Na]^+$ Calcd for $C_{12}H_{17}O_3NNaS$ 278.0814; found 278.0821.

(R_S)-N-(5-Bromo-2-hydroxy-3-methoxybenzylidene)-2-methyl-2-propanesulfinamide, **7j-(R_S)**. It was prepared following the general procedure from 2.36 g of (*R*)-*tert*-butanesulfinamide (19.5 mmol), 4.15 g of 5-bromo-2-hydroxy-3-methoxybenzaldehyde (18 mmol) and 10.4 mL of $Ti(OEt)_4$ (19.5 mmol). After 24 h, the resulting residue was purified by flash chromatography (EtOAc:hexane, 1:8) to give 4.73 g of **7j-(R_S)** (14.1 mmol, 78% yield) as a yellow solid; mp 130–133 °C; $[\alpha]_D^{20}$ +10.5 (*c* 1, $CHCl_3$); ^{1}H NMR (500 MHz, $CDCl_3$): δ 11.23 (bs, 1H), 8.63 (s, 1H), 7.24 (d, *J* = 2.2 Hz, 1H), 7.12 (d, *J* = 2.2 Hz, 1H), 3.92 (s, 3H), 1.25 (s, 9H) ppm; ^{13}C NMR (125 MHz, $CDCl_3$): δ 164.4, 149.6, 149.4, 126.3, 119.3, 119.1, 111.1, 58.3, 56.7, 22.4 ppm; HRMS (ESI) *m/z*: $[M + Na]^+$

Calcd for $C_{12}H_{18}O_3NBrNaS$ 355.9927; found 355.9926.

(R_S)-N-(5-Bromo-2-hydroxybenzylidene)-2-methyl-2-propanesulfinamide, **7k-(R_S)**. It was prepared following the general procedure from 2 g of (*R*)-*tert*-butanesulfinamide (16.5 mmol), 3.02 g of 5-bromosalicylaldehyde (15 mmol) and 3.46 mL of $Ti(OEt)_4$ (16.5 mmol). After 5 h, the resulting residue was purified by flash chromatography (EtOAc: hexane, 1:5) to give 3.12 g of **7k-(R_S)** (10.3 mmol, 69% yield) as a yellow solid; mp 90–93 °C; $[\alpha]_D^{20}$ − 61.4 (*c* 1, $CHCl_3$); ^{1}H NMR (500 MHz, $CDCl_3$): δ 11.04 (s, 1H), 8.63 (s, 1H), 7.59 (d, J = 2.5 Hz, 1H), 7.51 (dd, J = 2.5 and 8.8 Hz, 1H), 6.93 (d, J = 8.9 Hz, 1H), 1.26 (s, 9H) ppm; ^{13}C NMR (125 MHz, $CDCl_3$): δ 164.5, 159.4, 137.4, 135.3, 119.8, 119.5, 111.6, 58.2, 22.4 ppm; HRMS (ESI) *m/z*: $[M + Na]^+$ Calcd for $C_{11}H_{14}O_2NBrNaS$ 325.9815; found 325.9821.

(R_S)-N-(4-Diethylamino-2-hydroxybenzylidene)-2-methyl-2-propanesulfinamide, **7l-(R_S)**. It was prepared following the general procedure from 1.38 g of (*R*)-*tert*-butanesulfinamide (11.4 mmol), 2 g of 4-(diethylamino)-salicylaldehyde (10.3 mmol) and 3.27 mL of $Ti(OEt)_4$ (15.6 mmol). After 7 days, the resulting residue was purified by flash chromatography (EtOAc:hexane, 1:10) to give 1.70 g of **7l-(R_S)** (9.49 mmol, 82% yield) as an orange solid; mp 92–95 °C; $[\alpha]_D^{20}$ +123.3 (*c* 1, $CHCl_3$); ^{1}H NMR (500 MHz, $CDCl_3$): δ 11.29 (s, 1H), 8.48 (s, 1H), 7.23 (d, J = 8.8 Hz, 1H), 6.27 (dd, J = 2.5 and 8.8 Hz, 1H), 6.16 (d, J = 2.5 Hz, 1H), 3.40 (c, J = 7.2 Hz, 4H), 1.22 (s, 9H), 1.21 (t, J = 7.1 Hz, 6H) ppm; ^{13}C NMR (125 MHz, $CDCl_3$): δ 163.1, 162.7, 152.9, 135.1, 108.5, 104.4, 97.5, 57.4, 44.8, 22.3, 12.8 ppm; HRMS (ESI) *m/z*: $[M + H]^+$ Calcd for $C_{15}H_{25}O_2N_2S$ 297.1624; found 297.1631.

(R_S)-N-(2-Hydroxy-5-nitrobenzylidene)-2-methyl-2-propanesulfinamide, **7m-(R_S)** [25]. It was prepared following the general procedure from 2 g of (*R*)-*tert*-butanesulfinamide (16.5 mmol), 2.50 g of 2-hydroxy-5-nitrobenzaldehyde (15 mmol) and 3.46 mL of $Ti(OEt)_4$ (16.5 mmol). After 24 h, the resulting residue was purified by flash chromatography (EtOAc:hexane, 1:10) to give 2.09 g of **7m-(R_S)** (7.73 mmol, 52% yield) as an yellow solid; mp 144–147 °C; $[\alpha]_D^{20}$ − 108.6 (*c* 1, $CHCl_3$); ^{1}H NMR (500 MHz, $CDCl_3$): δ 11.88 (s, 1H), 8.78 (s, 1H), 8.46 (d, J = 2.8 Hz, 1H), 8.33 (dd, J = 2.8 and 9.2 Hz, 1H), 7.13 (d, J = 9.2 Hz, 1H), 1.29 (s, 9H) ppm; ^{13}C NMR (125 MHz, $CDCl_3$): δ 165.1, 164.2, 140.8, 129.5, 129.1, 118.4, 117.5, 58.4, 22.3 ppm; HRMS (ESI) *m/z*: $[M + H]^+$ Calcd for $C_{11}H_{15}O_4N_2S$ 271.0740; found 271.0747.

4.1.2. *Synthesis of tert-butylsulfinamides: general procedure [14d]*

To a solution of the corresponding *tert*-butylsulfinylimine (100 mol %) and ethyl acetate (400 mol%) in dry THF, at −78 °C under argon atmosphere, LHMDS 1 M (390 mol%) was added dropwise. Once the starting material was consumed, the reaction mixture is hydrolyzed with a saturated NH_4Cl aqueous solution. The aqueous phase was extracted with EtOAc (3 × 40 mL) and the combined organic phases were dried with anhydrous Na_2SO_4. The solvent was evaporated under reduced pressure and the reaction crude was purified by flash chromatography (EtOAc:hexane, 1:3) to obtain the desired compound.

(R_S,S_C)-Ethyl 3-(tert-butylsulfinamido)-3-(2-hydroxyphenyl)propanoate, **8a-(R_S,S_C)**. It was prepared following the general procedure from 440 mg of **7a-(R_S)** (1.95 mmol), 0.77 mL of ethyl acetate (7.81 mmol) and 7.62 mL of LHMDS (7.62 mmol). After 3.5 h, it is obtained 625.4 mg of **8a-(R_S,S_C)** (2 mmol, quantitative yield) as a low melting point yellow solid; $[\alpha]_D^{20}$ − 53.8 (*c* 1, $CHCl_3$); ^{1}H NMR (500 MHz, $CDCl_3$): δ 8.63 (bs, 1H), 7.16–7.11 (m, 2H), 6.86–6.80 (m, 2H), 5.29–5.28 (m, 1H), 4.92 (dt, J = 5.2 and 8.9 Hz, 1H), 4.12 (c, J = 7.0 Hz, 2H), 3.75 (AB fragment of an ABX system, $\Delta\nu$ = 1.69 ppm, J_{AX} = 5.2 Hz, J_{BX} = 8.9 Hz, J_{AB} = 16.3 Hz, 2H), 1.24 (s, 9H), 1.20 (t, J = 7.2 Hz, 3H) ppm; ^{13}C NMR (125 MHz, $CDCl_3$): δ 172.3, 155.5, 129.6, 128.8, 125.5, 120.2, 117.1, 61.3, 56.4, 54.4, 40.6, 22.9, 14.4 ppm; HRMS (ESI) *m/z*: $[M + H]^+$ Calcd for $C_{15}H_{24}O_4NS$ 314.1410; found 314.1421.

(S_S,R_C)-Ethyl 3-(tert-butylsulfinamido)-3-(2-hydroxyphenyl)propanoate, **8a-(S_S,R_C)**. It was prepared following the general procedure from 1 g of **7a-(S_S)** (4.44 mmol), 1.74 mL of ethyl acetate (17.75 mmol) and 17.31 mL of LHMDS (17.31 mmol). After 4 h, it is obtained 1.39 g of **8a-(S_S,R_C)** (4.43 mmol, quant. yield) as a low melting point yellow solid witj similar spectroscopic characteristics than **8a-(R_S,S_C)**; $[\alpha]_D^{20}$ +53.3 (*c* 1, $CHCl_3$) HRMS (ESI) *m/z*: $[M + H]^+$ Calcd for $C_{15}H_{24}O_4NS$ 314.1410; found 314.1421.

(R_S,S_C)-Ethyl 3-(tert-butylsulfinamido)-3-(2-naphthyl)propanoate, **8b-(R_S,S_C)**. It was prepared following the general procedure from 500 mg of **7b-(R_S)** (1.93 mmol), 86 μL of ethyl acetate (0.88 mmol) and 4.38 mL of LHMDS (4.38 mmol). After 24 min, it is obtained 499 mg of **8b-(R_S,S_C)** (1.43 mmol, 74% yield) as a white solid; mp 138 °C; $[\alpha]_D^{20}$ − 71.2 (*c* 1, $CHCl_3$); ^{1}H NMR (500 MHz, $CDCl_3$): δ 7.84–7.80 (m, 4H), 7.49–7.44 (m, 3H), 4.98–4.94 (m, 1H), 4.78 (d, J = 3.7 Hz, 1H) 4.13 (cd, J = 1.5 and 7.2 Hz, 2H), 2.94 (AB fragment of an ABX system, $\Delta\nu$ = 0.04 ppm, J_{AX} = 5.6 Hz, J_{BX} = 7.6 Hz, J_{AB} = 13.8 Hz, 2H), 1.24 (s, 9H), 1.22 (t, J = 7.2 Hz, 3H) ppm; ^{13}C NMR (125 MHz, $CDCl_3$): δ 138.1, 128.7, 128.2, 127.8, 126.8, 126.5, 126.4, 125.0, 61.2, 55.9, 42.4, 22.8, 14.3 ppm; HRMS (ESI) *m/z*: $[M + Na]^+$ Calcd for $C_{19}H_{25}O_3NNaS$ 370.1432; found 370.1447.

(R_S,R_C)-Ethyl 3-(tert-butylsulfinamido)-3-(2-naphthyl)propanoate, **8b-(R_S,R_C)**. It was prepared following the general procedure from 500 mg of **7b-(R_S)** (1.93 mmol), 86 μL of ethyl acetate (0.88 mmol) and 4.38 mL of LHMDS (4.38 mmol). After 24 min, it is obtained 74 mg of **8b-(R_S,R_C)** (0.21 mmol, 11% yield) as a yellow liquid; $[\alpha]_D^{20}$ − 24.6 (*c* 0.5, $CHCl_3$); ^{1}H NMR (500 MHz, $CDCl_3$): δ 7.85–7.81 (m, 4H), 7.51–7.47 (m, 3H), 5.05–5.01 (m, 1H), 4.14–4.04 (m, 2H), 3.98 (d, J = 5.2 Hz, 1H), 3.02 (AB fragment of an ABX system, $\Delta\nu$ = 0.22 ppm, J_{AX} = 6.2 Hz, J_{BX} = 7.9 Hz, J_{AB} = 15.6 Hz, 2H), 1.21 (s, 9H), 1.19 (t, J = 7.2 Hz, 3H) ppm; ^{13}C NMR (125 MHz, $CDCl_3$): δ 171.0, 138.3, 133.4, 133.3, 128.9, 128.3, 127.8, 126.5, 126.4, 126.3, 125.2, 60.9, 56.4, 56.3, 42.0, 22.7, 14.3 ppm; HRMS (ESI) *m/z*: $[M + Na]^+$ Calcd for $C_{19}H_{25}O_3NNaS$ 370.1430; found 370.1447.

(R_S,R_C,S_C,S_C,R_S)-N,N′-bis-(tert-Butylsulfinyl)-1,3-di-(2-naphthyl)-2-ethoxycarbonyl-1,3-diaminopropane, **9b-(R_S,R_C,S_C,S_C,R_S)**.

To a solution of 200 mg of *N-tert*-butylsulfinylimine **7b-(R_S)** (0.77 mmol) and 37.4 μL of ethyl acetate (0.39 mmol) in dry THF, at −78 °C under argon atmosphere, 1.92 mL of 1 M solution of LHMDS (1.92 mmol) is added dropwise. After 24 h, the starting material was consumed and the reaction mixture is hydrolyzed with a saturated NH_4Cl aqueous solution. The aqueous phase was extracted with EtOAc (3 × 40 mL) and the combined organic phases were dried with anhydrous Na_2SO_4. The solvent was evaporated under reduced pressure and the reaction crude was purified by flash chromatography (EtOAc:hexane, 1:3) to obtain the desired compound. The reaction crude was purified by flash chromatography (EtOAc:hexane, 1:2) to give 366.87 mg of **9b-(R_S,R_C,S_C,S_C,R_S)** (0.61 mmol, 79% yield) as a white solid. Mp 104 °C; $[\alpha]_D^{20}$ − 29.6 (*c* 1.0, $CHCl_3$); ^{1}H NMR (500 MHz, $CDCl_3$): δ 8.03 (s, 1H), 7.91–7.88 (m, 2H), 7.83–7.81 (m, 3H), 7.76–7.74 (m, 1H), 7.58 (s, 1H), 7.53–7.51 (m, 1H), 7.50–7.47 (m, 4H), 7.25 (dd, J = 1.7 and 8.6 Hz, 1H), 5.07 (d, J = 5.7 Hz, 1H), 4.86 (dd, J = 9.0 and 10.3 Hz, 1H), 4.64 (t, J = 5.8 Hz, 1H), 4.21 (t, J = 10.3 Hz, 1H), 4.17–4.02 (m, 2H), 3.43 (dd, J = 5.4 Hz and 8.5 Hz, 1H), 1.20 (s, 9H), 1.17 (s, 9H), 1.07 (t, J = 7.2 Hz, 3H) ppm; ^{13}C NMR (125 MHz, $CDCl_3$): δ 172.7, 138.1, 137.4, 133.6, 133.4, 133.3, 133.1, 129.2, 128.9, 128.6, 128.0, 127.9, 127.8, 127.7, 127.4, 124.6, 124.4, 61.5, 60.6, 59.0, 56.7, 56.3, 22.8, 22.7, 14.2 ppm; HRMS (ESI) *m/z*: $[M + Na]^+$ Calcd for $C_{34}H_{42}O_4N_2NaS_2$ 629.2451; found 629.2478.

(R_S,S_C)-Ethyl 3-(tert-butylsulfinamido)-3-(2-methylphenyl)propanoate, **8c-(R_S,S_C)**. It was prepared following the general procedure from 100 mg of **7c-(R_S)** (0.43 mmol), 42 μL of ethyl acetate (0.43 mmol) and 2.15 mL of LHMDS (2.15 mmol). After 45 min, it is obtained 45.1 mg of **8c-(R_S,S_C)** (0.15 mmol, 34% yield) as a low melting point brown solid; $[\alpha]_D^{20}$ − 280.2 (*c* 1, $CHCl_3$); ^{1}H NMR (500 MHz, $CDCl_3$): δ 7.32–7.31 (m, 1H), 7.20–7.14 (m, 3H), 5.04–5.01 (m, 1H), 4.60 (d, J = 4.0 Hz, 1H), 4.12 (c, J = 7.2 Hz, 2H), 2.81 (AB fragment of an ABX system, $\Delta\nu$ = 0.04 ppm, J_{AX} = 5.6 Hz, J_{BX} = 7.9 Hz, J_{AB} = 15.8 Hz, 2H), 2.42 (s, 3H), 1.22–1.98 (m, 12H) ppm; ^{13}C NMR (125 MHz, $CDCl_3$): δ 171.5, 138.6, 136.1, 130.8, 127.8, 126.8, 126.4, 61.0, 55.7, 51.4, 41.6, 22.7, 19.5,

14.2 ppm; HRMS (ESI) *m/z*: $[M + H]^+$ Calcd for $C_{16}H_{26}O_3NS$ 312.1628; found 312.1631.

(R_S,S_C)-Ethyl 3-(tert-butylsulfinamido)-3-(4-methoxyphenyl)propanoate, **8d-(R_S,S_C)**.

It was prepared following the general procedure from 100 mg of **7c-(R_S)** (0.42 mmol), 41 μL of ethyl acetate (0.42 mmol) and 2.09 mL of LHMDS (2.09 mmol). After 1 h, it is obtained 102 mg of **8d-(R_S,S_C)** (0.31 mmol, 74% yield) as a yellow solid; mp 98–99 °C; $[\alpha]_D^{20}$ − 56.8 (*c* 1, $CHCl_3$); ^{1}H NMR (500 MHz, $CDCl_3$): *δ* 7.26–7.24 (m, 2H), 6.88–6.86 (m, 2H), 4.76–4.72 (m, 1H), 4.61 (d, *J* = 3.9 Hz, 1H), 4.13 (dd, *J* = 1.5 and 7.2 Hz, 2H), 3.80 (s, 3H), 2.83–2.81 (m, 2H), 1.24–1.21 (s, 9H) ppm; ^{13}C NMR (125 MHz, $CDCl_3$): *δ* 171.5, 159.5, 138.8, 128.6, 114.2, 61.1, 55.7, 55.4, 55.1, 42.1, 22.8, 14.3 ppm; HRMS (ESI) *m/z*: $[M + Na]^+$ Calcd for $C_{16}H_{25}O_4NNaS$ 350.1391; found 350.1397.

(R_S,S_C)-Ethyl 3-(tert-butylsulfinamido)-3-(2-hydroxy-3-methylphenyl) propanoate, **8f-(R_S,S_C)**. It was prepared following the general procedure from 500 mg of **7f-(R_S)** (2.09 mmol), 0.82 mL of ethyl acetate (8.88 mmol) and 8.65 mL of LHMDS (8.65 mmol). After 2 h, it is obtained 514.2 mg of **8f-(R_S,S_C)** (1.57 mmol, 75% yield) as a low melting point yellow solid; $[\alpha]_D^{20}$ − 69.8 (*c* 1.0, $CHCl_3$); ^{1}H NMR (500 MHz, $CDCl_3$): *δ* 7.73 (s, 1H), 7.08 (d, *J* = 7.4 Hz, 1H), 6.99 (d, *J* = 7.6 Hz, 1H), 6.78 (t, *J* = 7.6 Hz, 1H), 5.26 (d, *J* = 2.9 Hz, 1H), 4.88–4.85 (m, 1H), 4.15 (ddd, *J* = 1.4, 7.1 and 13.8 Hz, 2H), 2.93 (AB fragment of an ABX system, Δ*ν* = 0.22 ppm, J_{AX} = 4.3 Hz, J_{BX} = 9.9 Hz, J_{AB} = 16.4 Hz, 2H), 2.23 (s, 3H), 1.26 (s, 9H), 1.24 (t, 7.2 Hz, 3H) ppm; ^{13}C NMR (125 MHz, $CDCl_3$): *δ* 172.1, 153.6, 131.2, 126.5, 126.3, 124.0, 120.3, 61.3, 55.9, 54.0, 39.4, 22.7, 16.0, 14.2 ppm; HRMS (ESI) *m/z*: $[M + Na]^+$ Calcd for $C_{16}H_{25}O_4NNaS$ 350.1392; found 350.1397.

(R_S,S_C)-Ethyl 3-(tert-butylsulfinamido)-3-(2-hydroxy-5-methylphenyl) propanoate, **8g-(R_S,S_C)**. It was prepared following the general procedure from 1 g of **7g-(R_S)** (4.18 mmol), 1.64 mL of ethyl acetate (16.7 mmol) and 16.28 mL of LHMDS (16.3 mmol). After 2 h, it is obtained 1.23 mg of **8g-(R_S,S_C)** (3.77 mmol, 90% yield) as a low melting point yellow solid; $[\alpha]_D^{20}$ − 50.5 (*c* 1.0, $CHCl_3$); ^{1}H NMR (500 MHz, $CDCl_3$): *δ* 8.02 (bs, 1H), 6.98–6.94 (m, 2H), 6.75 (d, *J* = 8.2 Hz, 1H), 5.26 (d, *J* = 4.5 Hz, 1H), 4.84–4.80 (m, 1H), 4.14 (c, *J* = 7.1 Hz, 2H), 2.96 (AB fragment of an ABX system, Δ*ν* = 0.19 ppm, J_{AX} = 4.9 Hz, J_{BX} = 9.3 Hz, J_{AB} = 16.2 Hz, 2H), 2.24 (s, 3H), 1.25 (s, 9H), 1.22 (t, *J* = 7.2 Hz, 3H) ppm; ^{13}C NMR (125 MHz, $CDCl_3$): *δ* 172.1, 153.0, 130.1, 129.5, 129.3, 124.6, 117.1, 61.1, 56.0, 54.5, 40.1, 22.7, 20.6, 14.2 ppm; HRMS (ESI) *m/z*: $[M + Na]^+$ Calcd for $C_{16}H_{25}O_4NNaS$ 350.1393; found 350.1397.

(R_S,S_C)-Ethyl 3-(tert-butylsulfinamido)-3-(2-hydroxy-4-methoxyphenyl) propanoate, **8h-(R_S,S_C)**. It was prepared following the general procedure from 1 g of **7h-(R_S)** (3.92 mmol), 1.54 mL of ethyl acetate (15.7 mmol) and 15.28 mL of LHMDS (15.3 mmol). After 3 h, it is obtained 1.33 mg of **8h-(R_S,S_C)** (3.89 mmol, quantitative yield) as a low melting point white solid; $[\alpha]_D^{20}$ − 57.1 (*c* 1.0, $CHCl_3$); ^{1}H NMR (500 MHz, $CDCl_3$): *δ* 8.81 (bs, 1H), 7.02 (d, *J* = 8.3 Hz, 1H), 6.39–6.36 (m, 2H), 5.21 (d, *J* = 4.9 Hz, 1H), 4.90–4.86 (m, 1H), 4.12 (c, *J* = 7.1 Hz, 2H), 3.70 (s, 3H), 2.98 (AB fragment of an ABX system, Δ*ν* = 0.13 ppm, J_{AX} = 5.4 Hz, J_{BX} = 8.9 Hz, J_{AB} = 16.1 Hz, 2H), 1.23 (s, 9H), 1.21 (t, 7.2 Hz, 3H) ppm; ^{13}C NMR (125 MHz, $CDCl_3$): *δ* 172.1, 160,7, 156.5, 129.1, 117.7, 105.8, 102.4, 61.0, 56.0, 52.3, 53.2, 40.6, 22.7, 14.2 ppm; HRMS (ESI) *m/z*: $[M + Na]^+$ Calcd for $C_{16}H_{25}O_5NNaS$ 366.1343; found 366.1346.

(R_S,S_C)-Ethyl 3-(tert-butylsulfinamido)-3-(2-hydroxy-5-methoxyphenyl) propanoate, **8i-(R_S,S_C)**. It was prepared following the general procedure from 500 mg of **7i-(R_S)** (2.22 mmol), 0.87 mL of ethyl acetate (8.88 mmol) and 8.65 mL of LHMDS (8.7 mmol). After 2 h, it is obtained 0.44 mg of **8i-(R_S,S_C)** (1.28 mmol, 58% yield) as a low melting point white solid; $[\alpha]_D^{20}$ − 52.4 (*c* 1.0, $CHCl_3$); ^{1}H NMR (500 MHz, $CDCl_3$): *δ* 8.01 (bs, 1H), 6.78–6.76 (m, 1H), 6.71–6.69 (m, 2H), 5.24 (d, *J* = 4.9 Hz, 1H), 4.88–4.85 (m, 1H), 4.13 (c, *J* = 7.1 Hz, 2H), 3.72 (s, 3H), 2.95 (AB fragment of an ABX system, Δ*ν* = 0.15 ppm, J_{AX} = 5.1 Hz, J_{BX} = 9.0 Hz, J_{AB} = 16.2 Hz, 2H), 1.24, (s, 9H), 1.22 (t, *J* = 7.0 Hz) ppm; ^{13}C NMR (125 MHz, $CDCl_3$): *δ* 172.0, 153.2, 149.0, 126.1, 117.8, 114.6, 114.0, 61.1, 56.1, 55.9, 54.0, 40.3, 22.7, 14.2 ppm; HRMS (ESI) *m/z*: $[M + Na]^+$ Calcd for $C_{16}H_{25}O_5NNaS$ 366.1342; found 366.1346.

(R_S,S_C)-Ethyl 3-(tert-butylsulfinamido)-3-(5-bromo-2-hydroxy-3-methoxyphenyl)propanoate, **8j-(R_S,S_C)**. It was prepared following the general procedure from 1 g of **7j-(R_S)** (3 mmol), 1.18 mL of ethyl acetate (12 mmol) and 11.7 mL of LHMDS (11.7 mmol). After 2.5 h, it is obtained 1.28 g of **8j-(R_S,S_C)** (3.05 mmol, quantitative yield) as a white solid; mp 117–119 °C; $[\alpha]_D^{20}$ − 36.0 (*c* 1.0, $CHCl_3$); ^{1}H NMR (500 MHz, $CDCl_3$): *δ* 7.00 (d, *J* = 2.2 Hz, 1H), 6.90 (d, *J* = 2.2 Hz, 1H), 5.01–4.97 (m, 1H), 4.85 (d, *J* = 6.3 Hz, 1H), 4.11 (c, *J* = 7.1 Hz, 2H), 3.87 (s, 3H), 2.94 (AB fragment of an ABX system, Δ*ν* = 0.05 ppm, J_{AX} = 5.7 Hz, J_{BX} = 7.2 Hz, J_{AB} = 15.9 Hz, 2H), 1.23–1.20 (m, 12H) ppm; ^{13}C NMR (125 MHz, $CDCl_3$): *δ* 171.4, 147.6, 142.6, 128.1, 123.2, 113.7, 111.6, 61.1, 56.5, 56.1, 52.2, 40.6, 22.8, 14.3 ppm; HRMS (ESI) *m/z*: $[M + Na]^+$ Calcd for $C_{16}H_{24}O_5NBrNaS$ 444.0452; found 444.0451.

(R_S,S_C)-Ethyl 3-(tert-butylsulfinamido)-3-(5-bromo-2-hydroxyphenyl) propanoate, **8k-(R_S,S_C)**. It was prepared following the general procedure from 500 mg of **7k-(R_S)** (1.64 mmol), 0.65 mL of ethyl acetate (6.57 mmol) and 6.40 mL of LHMDS (6.4 mmol). After 15 h, it is obtained 584 mg of **8k-(R_S,S_C)** (1.49 mmol, 91% yield) as a low melting point yellow solid; $[\alpha]_D^{20}$ − 54.4 (*c* 1.0, $CHCl_3$); ^{1}H NMR (500 MHz, $CDCl_3$): *δ* 8.81 (bs, 1H), 7.27–7.26 (m, 2H), 7.22 (dd, *J* = 2.5 and 8.6 Hz, 1H), 6.71 (d, *J* = 8.6 Hz, 1H), 5.24 (d, *J* = 4.5 Hz, 1H), 4.91–4.88 (m, 1H), 4.15 (c, *J* = 7.1 Hz, 2H), 2.90 (AB fragment of an ABX system, Δ*ν* = 0.10 ppm, J_{AX} = 5.1 Hz, J_{BX} = 9.0 Hz, J_{AB} = 16.1 Hz, 2H), 1.26 (s, 9H), 1.24 (t, 7.2 Hz, 3H) ppm; ^{13}C NMR (125 MHz, $CDCl_3$): *δ* 171.8, 154.5, 132.2, 131.2, 127.4, 118.8, 111.9, 61.3, 56.3, 52.7, 40.1, 22.8, 14.2 ppm; HRMS (ESI) *m/z*: $[M + Na]^+$ Calcd for $C_{15}H_{22}O_4NBrNaS$ 414.0343; found 414.0345.

(R_S,S_C)-Ethyl 3-(tert-butylsulfinamido)-3-(4-diethylamino-2-hydroxyphenyl)propanoate, **8l-(R_S,S_C)**. It was prepared following the general procedure from 500 mg of **7l-(R_S)** (1.69 mmol), 0.66 mL of ethyl acetate (6.74 mmol) and 6.58 mL of LHMDS (6.6 mmol). After 20 h, it is obtained 540.7 mg of **8l-(R_S,S_C)** (1.40 mmol, 83% yield) as a yellow solid; mp 58 °C; $[\alpha]_D^{20}$ − 54.5 (*c* 1.0, $CHCl_3$); ^{1}H NMR (500 MHz, $CDCl_3$): *δ* 7.90 (bs, 1H), 6.95 (d, *J* = 8.5 Hz, 1H), 6.25–6.20 (m, 2H), 5.18 (d, *J* = 3.6 Hz, 1H), 4.79–4.15 (m, 1H), 4.14 (c, *J* = 7.1 Hz, 2H), 3.30 (c, *J* = 7.1 Hz, 4H), 2.92 (AB fragment of an ABX system, Δ*ν* = 0.18 ppm, J_{AX} = 4.6 Hz, J_{BX} = 9.5 Hz, J_{AB} = 16.3 Hz, 2H), 1.27–1.24 (m, 12H), 1.14 (t, *J* = 7.1 Hz, 6H) ppm; ^{13}C NMR (125 MHz, $CDCl_3$): *δ* 172.2, 156.5, 129.5, 104.4, 100.7, 96.7, 61.0, 55.6, 53.2, 40.1, 31.2, 22.7, 14.1, 12.6 ppm; HRMS (ESI) *m/z*: $[M + H]^+$ Calcd for $C_{19}H_{33}O_4N_2S$ 385.2155; found 385.2156.

(R_S,S_C)-Ethyl 3-(tert-butylsulfinamido)-3-(2-hydroxy-5-nitrophenyl) propanoate, **8m-(R_S,S_C)**. It was prepared following the general procedure from 1 g of **7m-(R_S)** (3.70 mmol), 1.5 mL of ethyl acetate (14.8 mmol) and 14.41 mL of LHMDS (14.4 mmol). After 2 h, it is obtained 1.22 g of **8m-(R_S,S_C)** (3.39 mmol, 92% yield) as a yellow solid; mp 90–92 °C; $[\alpha]_D^{20}$ − 79.2 (*c* 1.0, $CHCl_3$); ^{1}H NMR (500 MHz, $CDCl_3$): *δ* 10.75 (bs, 1H), 8.16 (d, *J* = 2.8 Hz, 1H), 7.98 (dd, *J* = 2.8 and 8,9 Hz, 1H), 6.79 (d, *J* = 9 Hz, 1H), 5.31 (d, *J* = 3.9 Hz, 1H), 5.16–5.12 (m, 1H), 4.18 (ddd, *J* = 0.7, 7.2 and 14.3 Hz, 2H), 2.87–2.85 (m, 2H), 1.31 (s, 9H), 1.26 (t, *J* = 7.1 Hz, 3H) ppm; ^{13}C NMR (125 MHz, $CDCl_3$): *δ* 171.6, 161.3, 140.7, 126.4, 125.5, 124.6, 116.3, 61.4, 56.6, 50.2, 40.0, 22.8, 14.2 ppm; HRMS (ESI) *m/z*: $[M + Na]^+$ Calcd for $C_{15}H_{22}O_6N_2NaS$ 381.1091; found 381.1091.

4.1.3. *Synthesis of -N-(tert-butylsulfinyl)-4-amino-3,4-dihydrocoumarins: general procedure*

To a solution of the corresponding *tert*-butylsulfinamide (100 mol%) in dry dichloromethane, at 0 °C under argon atmosphere, BF_3OEt_2 (1000 mol%) was added. Once the starting material was consumed (24 hours), the reaction mixture is hydrolyzed with a saturated $NaHCO_3$ aqueous solution. The aqueous phase was extracted with CH_2Cl_2 (3 × 40 mL) and the combined organic phases were washed with a saturated NaCl aqueous solution and dried with anhydrous Na_2SO_4. The solvent was evaporated and the desired compound is obtained with no further purification.

(R_S,S_C)–N-(tert-Butylsulfinyl)-4-amino-3,4-dihydrocoumarin, **10a-(R_S,**

S_C). It was prepared following the general procedure from 500 mg of **8a-(R_S,S_C)** (1.60 mmol), 75 mL of dichloromethane and 2.95 mL of BF_3OEt_2 (23.9 mmol). After 24 h, it is obtained 364.8 mg of **10a-(R_S,S_C)** (1.40 mmol, 88% yield) as a green solid; mp 61–63 °C; $[\alpha]_D^{20}$ − 71.1 (*c* 1.0, $CHCl_3$); ^{1}H NMR (500 MHz, $CDCl_3$): δ 7.45–7.47 (m, 1H), 7.40–7.37 (m, 1H), 7.20–7.18 (m, 1H), 7.12–7.10 (d, J = 8.1 Hz, 1H), 4.76 (c, J = 4.6 Hz, 1H), 3.46 (d, J = 4.5 Hz, 1H), 3.02 (AB fragment of an ABX system, $\Delta\nu$ = 0.19 ppm, J_{AX} = 5.0 Hz, J_{BX} = 4.2 Hz, J_{AB} = 15.9 Hz, 2H), 1.15 (s, 9H) ppm; ^{13}C NMR (125 MHz, $CDCl_3$): δ 166.1, 151.5, 130.6, 129.0, 124.7, 122.3, 117.6, 59.3, 50.1, 37.9, 22.6 ppm; HRMS (ESI) *m/z*: $[M + Na]^+$ Calcd for $C_{13}H_{17}O_3NNaS$ 290.0814; found 290.0821.

(R_S,S_C)–N-(tert-Butylsulfinyl)-4-amino-8-methyl-3,4-dihydrocoumarin, **10f-(R_S,S_C)**. It was prepared following the general procedure from 200 mg of **8f-(R_S,S_C)** (0.61 mmol), 75 mL of dichloromethane and 0.75 mL of BF_3OEt_2 (6.1 mmol). After 24 h, it is obtained 172 mg of **10f-(R_S,S_C)** (0.61 mmol, quantitative yield) as a white solid; mp 154–156 °C; $[\alpha]_D^{20}$ − 99.8 (*c* 1.0, $CHCl_3$); ^{1}H NMR (500 MHz, $CDCl_3$): δ 7,27 (d, J = 7.6 Hz, 1H), 7.23 (d, J = 7.6 Hz, 1H), 7.08 (t, J = 7.6 Hz, 1H), 4.73 (c, J = 4.7 Hz, 1H), 3.47 (d, J = 4.6 Hz, 1H), 3.00 (AB fragment of an ABX system, $\Delta\nu$ = 0.16 ppm, J_{AX} = 5.0 Hz, J_{BX} = 4.2 Hz, J_{AB} = 15.9 Hz, 2H), 2.32 (s, 3H), 1.14 (s, 9H) ppm; ^{13}C NMR (125 MHz, $CDCl_3$): δ 166.4, 149.7, 132.1, 126.9, 126.5, 124.2, 122.1, 56.3, 50.3, 37.8, 22.6, 15,8 ppm; HRMS (ESI) *m/z*: $[M + Na]^+$ Calcd for $C_{14}H_{19}O_3NNaS$ 304.0966; found 304.0978.

(R_S,S_C)–N-(tert-Butylsulfinyl)-4-amino-6-methyl-3,4-dihydrocoumarin, **10g-(R_S,S_C)**. It was prepared following the general procedure from 200 mg of **8g-(R_S,S_C)** (0.61 mmol), 75 mL of dichloromethane and 0.75 mL of BF_3OEt_2 (6.1 mmol). After 24 h, it is obtained 164.8 mg of **10g-(R_S,S_C)** (0.59 mmol, 96% yield) as a brown solid; mp 143–145 °C; $[\alpha]_D^{20}$ − 48.7 (*c* 1.0, $CHCl_3$); ^{1}H NMR (500 MHz, $CDCl_3$): δ 7.24 (d, J = 1.5 Hz, 1H), 7.17 (dd, J = 1.7 and 8.3 Hz, 1H), 6.99 (d, J = 8.3 Hz, 1H), 4.70 (c, J = 4.5 Hz, 1H), 3.46 (d, J = 4.4 Hz, 1H), 2.98 (AB fragment of an ABX system, $\Delta\nu$ = 0.15 ppm, J_{AX} = 4.8 Hz, J_{BX} = 4.2 Hz, J_{AB} = 16.0 Hz, 2H), 2.36 (s, 3H), 1.15 (s, 9H) ppm; ^{13}C NMR (125 MHz, $CDCl_3$): δ 166.4, 149.4, 134.4, 131.1, 129.4, 121.9, 117.3, 56.2, 50.1, 37.9, 22.6, 20.9 ppm; HRMS (ESI) *m/z*: $[M + Na]^+$ Calcd for $C_{14}H_{19}O_3NNaS$ 304.0966; found 304.0978.

(R_S,S_C)–N-(tert-Butylsulfinyl)-4-amino-6-methoxy-3,4-dihydrocoumarin, **10i-(R_S,S_C)**. It was prepared following the general procedure from 200 mg of **8i-(R_S,S_C)** (0.58 mmol), 75 mL of dichloromethane and 0.2 mL of BF_3OEt_2 (5.8 mmol). After 24 h, it is obtained 172.7 mg of **10i-(R_S,S_C)** (0.58 mmol, quantitative yield) as a low melting point black solid; $[\alpha]_D^{20}$ − 27.4 (*c* 1.0, $CHCl_3$); ^{1}H NMR (500 MHz, $CDCl_3$): δ 7.03 (d, J = 8.9 Hz, 1H), 6.97 (d, J = 3.0 Hz, 1H), 6,89 (dd, J = 3.0 and 8.9 Hz, 1H), 4.70 (c, J = 5.0 Hz, 1H), 3.82 (s, 3H), 3.47 (d, J = 5.0 Hz, 1H), 2.99 (AB fragment of an ABX system, $\Delta\nu$ = 0.20 ppm, J_{AX} = 4.3 Hz, J_{BX} = 5.4 Hz, J_{AB} = 16.1 Hz, 2H), 1.16 (s, 9H) ppm; ^{13}C NMR (125 MHz, $CDCl_3$): δ 166.4, 156.4, 145.2, 123.4, 118.4, 115.7, 113.7, 56.4, 56.0, 50.4, 37.9, 22.6 ppm; HRMS (ESI) *m/z*: $[M + Na]^+$ Calcd for $C_{14}H_{19}O_3NNaS$ 320.0914; found 320.0927.

(R_S,S_C)-6-Bromo-N-(tert-butylsulfinyl)-4-amino-8-methoxy-3,4-dihydrocoumarin, **10j-(R_S,S_C)**. It was prepared following the general procedure from 200 mg of **8j-(R_S,S_C)** (0.48 mmol), 75 mL of dichloromethane and 5.9 mL of BF_3OEt_2 (47.5 mmol). After 12 days, it is obtained 175.6 mg of **10j-(R_S,S_C)** (0.47 mmol, quantitative yield) as a brown solid; mp 79–80 °C; $[\alpha]_D^{20}$ − 70.4 (*c* 1.0, $CHCl_3$); ^{1}H NMR (500 MHz, $CDCl_3$): δ 7.18 (d, J = 2.0 Hz, 1H), 7.09 (d, J = 2.2 Hz, 1H), 4.70 (c, J = 5.0 Hz, 1H), 3.89 (s, 3H), 3.47 (d, J = 5.2 Hz, 1H), 3.00 (AB fragment of an ABX system, $\Delta\nu$ = 0.20 ppm, J_{AX} = 5.5 Hz, J_{BX} = 4.3 Hz, J_{AB} = 16.0 Hz, 2H), 1.18 (s, 9H) ppm; ^{13}C NMR (125 MHz, $CDCl_3$): δ 164.8, 148.8, 140.0, 125.1, 122.7, 117.2, 116.7, 56.6, 50.2, 37.6, 29.8, 22.6 ppm; HRMS (ESI) *m/z*: $[M + Na]^+$ Calcd for $C_{14}H_{18}O_4NBrNaS$ 398.0017; found 398.0032.

(R_S,S_C)-6-Bromo-N-(tert-butylsulfinyl)-4-amino-3,4-dihydrocoumarin, **10k-(R_S,S_C)**. It was prepared following the general procedure from 200 mg of **8k-(R_S,S_C)** (0.51 mmol), 75 mL of dichloromethane and 0.63 mL of BF_3OEt_2 (5.1 mmol). After 24 h, it is obtained 127.9 mg of **10k-(R_S,S_C)** (0.37 mmol, 80% yield) as a green solid; mp 68–70 °C; $[\alpha]_D^{20}$ − 33.7 (*c* 1.0, $CHCl_3$); ^{1}H NMR (500 MHz, $CDCl_3$): δ 7.58 (d, J = 2.4 Hz, 1H), 7.50–7.48 (dd, J = 2.4 and 8.6 Hz, 1H), 6.99 (d, J = 8.6 Hz, 1H), 4.72 (c, J = 5.0 Hz, 1H), 3.59 (d, J = 5.1 Hz, 1H), 3.02 (AB fragment of an ABX system, $\Delta\nu$ = 0.18 ppm, J_{AX} = 5.6 Hz, J_{BX} = 4.3 Hz, J_{AB} = 16.1 Hz, 2H), 1.17 (s, 9H) ppm; ^{13}C NMR (125 MHz, $CDCl_3$): δ 165.4, 150.5, 133.5, 131.5, 124.7, 119.3, 117.3, 56.6, 50.0, 37.5, 22.6 ppm; HRMS (ESI) *m/z*: $[M + Na]^+$ Calcd for $C_{13}H_{16}O_3NBrNaS$ 367.9920; found 367.9926.

(R_S,S_C)-7-Diethylamino-N-(tert-butylsulfinyl)-4-amino-3,4-dihydrocoumarin, **10l-(R_S,S_C)**. It was prepared following the general procedure from 200 mg of **8l-(R_S,S_C)** (0.52 mmol), 75 mL of dichloromethane and 10.24 mL of BF_3OEt_2 (83.2 mmol). After 7 days, it is obtained 131.9 mg of **10l-(R_S,S_C)** (0.39 mmol, 75% yield) as a green solid; mp 70–72 °C; $[\alpha]_D^{20}$ − 15.5 (*c* 0.125, $CHCl_3$); ^{1}H NMR (500 MHz, $CDCl_3$): δ 7.22–7.21 (d, J = 8.6 Hz, 1H), 6.42 (dd, J = 2.6 and 8.6 Hz, 1H), 6.33 (d, J = 2.6 Hz, 1H), 4.64 (c, J = 4.3 Hz, 1H), 3.51 (d, J = 4.4 Hz, 1H), 3.34 (c, J = 7.1 Hz, 4H), 2.95 (AB fragment of an ABX system, $\Delta\nu$ = 0.13 ppm, J_{AX} = 4.2 Hz, J_{BX} = 4.2 Hz, J_{AB} = 16.0 Hz, 2H), 1.16 (t, J = 7.1 Hz, 6H), 1.14 (s, 9H) ppm; ^{13}C NMR (125 MHz, $CDCl_3$): δ 167.1, 152.9, 149.6, 129.9, 107.7, 107.5, 99.7, 56.0, 49.7, 44.6, 38.5, 22.6, 12.6 ppm; HRMS (ESI) *m/z*: $[M + H]^+$ Calcd for $C_{17}H_{26}O_3N_2S$ 339.1728; found 339.1737.

(R_S,S_C)–N-(tert-Butylsulfinyl)-4-amino-6-nitro-3,4-dihydrocoumarin, **10m-(R_S,S_C)**. It was prepared following the general procedure from 200 mg of **8m-(R_S,S_C)** (0.56 mmol), 75 mL of dichloromethane and 11.4 mL of BF_3OEt_2 (89.6 mmol). After 7 days, it is obtained 175.4 mg of **10m-(R_S,S_C)** (0.56 mmol, quantitative yield) as an orange solid; mp 68–70 °C; $[\alpha]_D^{20}$ − 94.7 (*c* 0.25, $CHCl_3$); ^{1}H NMR (500 MHz, $CDCl_3$): δ 8.41 (d, J = 2.7 Hz, 1H), 8.30 (dd, J = 2.7 and 8.9 Hz, 1H), 7.28 (s, 1H), 4.89 (c, J = 5.5 Hz, 1H), 3.70 (d, J = 5.6 Hz, 1H), 3.14 (AB fragment of an ABX system, $\Delta\nu$ = 0.22 ppm, J_{AX} = 6.3 Hz, J_{BX} = 4.5 Hz, J_{AB} = 16.2 Hz, 2H), 1.22 (s, 9H) ppm; ^{13}C NMR (125 MHz, $CDCl_3$): δ 164.2, 155.6, 144.5, 126.3, 124.5, 124.2, 118.6, 56.9, 50.1, 37.3, 22.6 ppm; HRMS (ESI) *m/z*: $[M + H]^+$ Calcd for $C_{13}H_{17}O_5N_2S$ 313.0780; found 313.0813.

4.1.4. ***Desulfinylation of tert-butylsulfinamides.*** *General procedure*

To a solution of the corresponding *tert*-butylsulfinamide (100 mol%) in dry ethyl acetate, at 0 °C under argon atmosphere, a 4 N solution of HCl in dioxane (150 mol% for each sulfinyl group) is added dropwise. Once the starting material was consumed, the precipitate is filtered and washed with diethyl ether, to give the pure desired compound.

(S_C)-4-Amino-3,4-dihydrocoumarin hydrochloride, **11a-(S_C)**. It was prepared following the general procedure from 200 mg of **10a-(R_S,S_C)** (0.77 mmol), and 0.29 mL of 4 N HCl/dioxane (1.15 mmol). After 24 h days, it is obtained 144.0 mg of **11a-(S_C)** (0.72 mmol, 94% yield) as a white solid; mp 94 °C; $[\alpha]_D^{20}$ +12.0 (*c* 1, MeOH); ^{1}H NMR (500 MHz, MeOD): δ 7.27–7.24 (m, 2H), 6.92–6.88 (m, 2H), 4.81, (dd, J = 5.9 and 8.0 Hz, 1H), 3.12 (AB fragment of an ABX system, $\Delta\nu$ = 0.14 ppm, J_{AX} = 6.0 Hz, J_{BX} = 8.2 Hz, J_{AB} = 17.0 Hz, 2H) ppm; ^{13}C NMR (125 MHz, MeOD): δ 172.2, 156.5, 131.8, 129.8, 122.9, 121.1, 116.9, 50.6, 37.6 ppm. HRMS (ESI) *m/z*: $[M + H]^+$ Calcd for $C_9H_{10}NO_2$ 163.0633; found 163.0633.

(S_C)-4-Amino-6-methoxy-3,4-dihydrocoumarin hydrochloride, **11i-(S_C)**. It was prepared following the general procedure from 50 mg of **10i-(R_S,S_C)** (0.17 mmol), and 63 μL of 4 N HCl/dioxane (0.25 mmol). After 24 h, it is obtained 27.7 mg of **11i-(S_C)** (0.12 mmol, 70% yield) as a black liquid; ^{1}H NMR (500 MHz, MeOD): δ 6.87–6.86 (m, 1H), 6.85–6.82 (m, 2H), 4.76 (dd, J = 8.3 and 5.9 Hz, 1H), 3.75 (s, 3H), 3.08 (AB fragment of an ABX system, $\Delta\nu$ = 0.16 ppm, J_{AX} = 8.3 Hz, J_{BX} = 5.9 Hz, J_{AB} = 17.3 Hz, 2H) ppm; ^{13}C NMR (125 MHz, MeOD): δ 173.4, 154.5, 150.1, 123.5, 117.6, 116.8, 115.3, 56.3, 50.5, 37.4 ppm; HRMS (ESI) *m/z*: $[M + H]^+$ Calcd for $C_{10}H_{12}O_3N$ 194.0739; found 194.0742.

(S_C)-4-Amino-6-bromo-8-methoxy-3,4-dihydrocoumarin hydrochloride, **11j-(S_C)**. It was prepared following the general procedure from 320 mg of **10j-(R_S,S_C)** (0.87 mmol), and 330 μL of 4 N HCl/dioxane (1.3 mmol).

After 24 h, it is obtained 159.7 mg of **11i-(S_C)** (0.52 mmol, 60% yield) as a black liquid; ^{1}H NMR (500 MHz, MeOD): δ 7.12–7.09 (m, 2H), 4.85–4.83 (m, 1H), 3.88 (s, 3H), 3.08 (AB fragment of an ABX system, $\Delta\nu = 0.15$ ppm, $J_{AX} = 8.0$ Hz, $J_{BX} = 5.6$ Hz, $J_{AB} = 16.9$ Hz, 2H) ppm; ^{13}C NMR (125 MHz, MeOD): δ 173.1, 150.1, 145.1, 124.6, 123.6, 116.5, 112.1, 57.1, 49.3, 37.2 ppm; HRMS (ESI) *m/z*: $[M + H]^+$ Calcd for $C_{10}H_{11}BrNO_3$ 270.9844; found 270.9844.

(S_C)-4-Amino-6-bromo-3,4-dihydrocoumarin hydrochloride, **11k-(S_C)**. It was prepared following the general procedure from 115 mg of **10k-(R_S,S_C)** (0.35 mmol), and 120 μL of 4 N HCl/dioxane (0.5 mmol). After 24 h, it is obtained 53.7 mg of **11k-(S_C)** (0.19 mmol, 58% yield) as a brown solid; mp 102–103 °C; $[\alpha]_D^{20}$ +32.0 (*c* 1, MeOH); ^{1}H NMR (500 MHz, MeOD): δ 7.48 (d, $J = 2.5$ Hz, 1H), 7.40 (dd, $J = 2.4$ and 8.6 Hz, 1H), 6.90 (d, $J = 8.6$ Hz, 1H), 4.80 (dd, $J = 6.2$ and 7.8 Hz, 1H), 3.11 (AB fragment of an ABX system, $\Delta\nu = 0.14$ ppm, $J_{AX} = 8.0$ Hz, $J_{BX} = 6.1$ Hz, $J_{AB} = 17.2$ Hz, 2H) ppm; ^{13}C NMR (125 MHz, MeOD): δ 173.2, 155.8, 134.3, 132.6, 125.3, 118.8, 112.4, 49.9, 37.2 ppm; HRMS (ESI) *m/z*: $[M + H]^+$ Calcd for $C_9H_9BrNO_2$ 241.9738; found 241.9739.

(S_C)-4-Amino-7-diethylamino-3,4-dihydrocoumarin hydrochloride, **11l-(S_C)**. It was prepared following the general procedure from 170 mg of **10l-(R_S,S_C)** (0.5 mmol), and 190 μL of 4 N HCl/dioxane (0.75 mmol). After 24 h, it is obtained 127.4 mg of **11l-(S_C)** (0.5 mmol, quant. yield) as a dark brown liquid; ^{1}H NMR (500 MHz, MeOD): δ 7.57 (d, $J = 8.4$ Hz, 1H), 7.22 (d, $J = 2.1$ Hz, 1H), 7.18 (dd, $J = 2.2$ and 8.3 Hz, 1H), 4.89 (t, $J = 6.5$ Hz, 1H), 3.66 (c, $J = 7.2$ Hz, 4H), 3.12 (AB fragment of an ABX system, $\Delta\nu = 0.13$ ppm, $J_{AX} = 8.0$ Hz, $J_{BX} = 6.2$ Hz, $J_{AB} = 17.3$ Hz, 2H), 1.17 (t, $J = 7.2$ Hz, 6H) ppm; ^{13}C NMR (125 MHz, MeOD): δ 173.0, 158.2, 140.2, 132.3, 125.9, 114.4, 111.2, 54.8, 37.0, 25.8, 10.7 ppm; HRMS (ESI) *m/z*: $[M + H]^+$ Calcd for $C_{13}H_{19}O_2N_2$ 235.1368; found 235.1402.

(S_C)-4-Amino-6-nitro-3,4-dihydrocoumarin hydrochloride, **11m-(S_C)**. It was prepared following the general procedure from 160 mg of **10m-(R_S, S_C)** (0.51 mmol), and 0.19 mL of 4 N HCl/dioxane (0.77 mmol). After 24 h, it is obtained 97.6 mg of **11m-(S_C)** (0.40 mmol, 79% yield) as a black liquid; ^{1}H NMR (500 MHz, MeOD): δ 8.30 (d, $J = 2.4$ Hz, 1H), 8.20 (dd, $J = 2.5$ and 9.0 Hz, 1H), 7.08 (d, $J = 9.0$ Hz, 1H), 4.92 (t, $J = 6.9$ Hz, 1H), 3.12 (AB fragment of an ABX system, $\Delta\nu = 0.10$ ppm, $J_{AX} = 7.9$ Hz, $J_{BX} = 5.7$ Hz, $J_{AB} = 17.3$ Hz, 2H) ppm; ^{13}C NMR (125 MHz, MeOD): δ 173.0, 162.4, 141.9, 127.7, 126.2, 124.2, 117.1, 49.5, 37.0 ppm; HRMS (ESI) *m/z*: $[M + H]^+$ Calcd for $C_9H_9O_4N_2$ 209.0484; found 209.0518.

(S_C)-Ethyl 3-amino-3-(2-hydroxyphenyl)propanoate hydrochloride, **12a-(S_C)**. It was prepared following the general procedure from 585.4 mg of **8a-(R_S,S_C)** (1.87 mmol) and 0.71 mL of 4 N HCl (2.80 mmol). After 4.5 h, it is obtained 378.2 of **12a-(S_C)** (1.80 mmol, 96% yield) as a white solid; mp 169–170 °C; $[\alpha]_D^{20}$ − 18.4 (*c* 1, MeOH); ^{1}H NMR (500 MHz, MeOD): δ 7.26–7.24 (m, 2H), 6.93–6.87 (m, 2H), 4.83–4.80, (m, 1H), 4.18–4.12 (m, 2H), 3.12(AB fragment of an ABX system, $\Delta\nu = 0.13$ ppm, $J_{AX} = 6.5$ Hz, $J_{BX} = 7.9$ Hz, $J_{AB} = 16.8$ Hz, 2H), 1.22 (t, $J = 7.1$ Hz, 3H) ppm; ^{13}C NMR (125 MHz, MeOD): δ 171.7, 156.5, 131.8, 129.9, 122.8, 121.0, 116.9, 62.3, 50.5, 37.8, 14.4 ppm. HRMS (ESI) *m/z*: $[M + H]^+$ Calcd for $C_{11}H_{16}O_3N$ 210.1118; found 210.1125.

(S_C)-Ethyl 3-amino-3-(2-hydroxyphenyl)propanoate hydrochloride, **12a-(R_C)**. It was prepared following the general procedure from 420 mg of **8a-(S_S,R_C)** (1.34 mmol) and 0.50 mL of 4 N HCl (2.01 mmol). After 4.5 h, it is obtained 312.8 mg of **12a-(R_C)** (1.27 mmol, 95% yield) as a white solid with similar spectroscopis characteristics than **12a-(S_C)**; mp 170–171 °C; $[\alpha]_D^{20}$ +18.9 (*c* 1, MeOH); HRMS (ESI) *m/z*: $[M + H]^+$ Calcd for $C_{11}H_{16}O_3N$ 210.1118; found 210.1125.

(S_C)-Ethyl 3-amino-2-(2-hydroxy-4-methoxyphenyl) propanoate hydrochloride, **12h-(S_C)**. It was prepared following the general procedure from 300 mg of **8h-(R_S,S_C)** (0.87 mmol), and 320 μL of 4 N HCl/dioxane (1.31 mmol). After 24 h, it is obtained 187.3 mg of **12h-(S_C)** (0.68 mmol, 78% yield) as a dark brown liquid; ^{1}H NMR (500 MHz, MeOD): δ 6.86–6.84 (m, 3H), 4.78–4.76 (m, 1H), 4.16 (cd, $J = 1.0$ and 7.2 Hz, 2H), 3.74 (s, 3H), 3.10 (AB fragment of an ABX system, $\Delta\nu = 0.12$ ppm, $J_{AX} = 7.9$ Hz, $J_{BX} = 6.4$ Hz, $J_{AB} = 16.8$ Hz, 2H), 1.23 (t, $J = 7.1$ Hz, 3H) ppm; ^{13}C NMR (125 MHz, MeOD): δ 171.6, 154.5, 150.1, 123.3, 117.6, 116.9, 115.4, 62.3, 56.3, 50.5, 37.8, 14.3 ppm; HRMS (ESI) *m/z*: $[M + H]^+$ Calcd for $C_{12}H_{18}O_4N$ 240.1230; found 240.1229.

(S_C)-Ethyl 3-amino-2-(2-hydroxy-5-methoxyphenyl) propanoate hydrochloride, **12i-(S_C)**. It was prepared following the general procedure from 300 mg of **8i-(R_S,S_C)** (0.87 mmol), and 320 μL of 4 N HCl/dioxane (1.31 mmol). After 24 h, it is obtained 215.5 mg of **12i-(S_C)** (0.78 mmol, 90% yield) as a dark brown liquid; ^{1}H NMR (500 MHz, MeOD): δ 7.16 (d, $J = 8.5$ Hz, 1H), 6.49 (d, $J = 2.4$ Hz, 1H), 6.46 (dd, $J = 2.4$ and 8.5 Hz, 1H), 4.76 (t, $J = 7.2$ Hz, 1H), 4.14 (cd, $J = 1.6$ and 7.1 Hz, 2H), 3.76 (s, 3H), 3.10 (AB fragment of an ABX system, $\Delta\nu = 0.13$ ppm, $J_{AX} = 7.8$ Hz, $J_{BX} = 6.8$ Hz, $J_{AB} = 16.7$ Hz, 2H), 1.22 (t, $J = 7.1$ Hz, 3H) ppm; ^{13}C NMR (125 MHz, MeOD): δ 171.7, 163.2, 157.6, 130.7, 115.2, 106.4, 102.7, 62.2, 55.8, 50.1, 37.9, 14.4 ppm; HRMS (ESI) *m/z*: $[M + H]^+$ Calcd for $C_{12}H_{18}O_4N$ 240.1230; found 240.1232.

(S_C)-Ethyl 3-amino-2-(5-bromo-2-hydroxy-3-methoxyphenyl) propanoate hydrochloride, **12j-(S_C)**. It was prepared following the general procedure from 900 mg of **8j-(R_S,S_C)** (2.13 mmol), and 810 μL of 4 N HCl/dioxane (3.18 mmol). After 24 h, it is obtained 442.0 mg of **12j-(S_C)** (1.25 mmol, 59% yield) as a dark brown liquid; ^{1}H NMR (500 MHz, MeOD): δ 7.13 (d, $J = 2.2$ Hz, 1H), 7.07 (d, $J = 2.2$ Hz, 1H), 4.86–4.85 (m, 1H), 4.15 (cd, $J = 2.2$ and 7.2 Hz, 2H), 3.88 (s, 3H), 3.08 (AB fragment of an ABX system, $\Delta\nu = 0.12$ ppm, $J_{AX} = 7.7$ Hz, $J_{BX} = 6.7$ Hz, $J_{AB} = 16.7$ Hz, 2H), 1.21 (t, $J = 7.2$ Hz, 3H) ppm; ^{13}C NMR (125 MHz, MeOD): δ 171.3, 150.2, 145.3, 124.4, 123.7, 116.6, 112.1, 62.3, 57.0, 49.3, 37.6, 14.3 ppm; HRMS (ESI) *m/z*: $[M + H]^+$ Calcd for $C_{12}H_{17}O_4NBr$ 318.0335; found 318.0332.

(S_C)-Ethyl 3-amino-2-(2-hydroxy-5-bromophenyl) propanoate hydrochloride, **12k-(S_C)**. It was prepared following the general procedure from 430 mg of **8k-(R_S,S_C)** (1.10 mmol), and 410 μL of 4 N HCl/dioxane (1.64 mmol). After 24 h, it is obtained 90.8 mg of **12k-(S_C)** (0.28 mmol, 25% yield) as a dark brown liquid; ^{1}H NMR (500 MHz, MeOD): δ 7.44 (d, $J = 2.20$ Hz, 1H), 7.37 (dd, $J = 2.0$ and 8.6 Hz, 1H), 6.89 (d, $J = 8.6$ Hz, 1H), 4.15 (cd, $J = 1.4$ and 6.9 Hz, 2H), 3.12 (AB fragment of an ABX system, $\Delta\nu = 0.11$ ppm, $J_{AX} = 7.4$ Hz, $J_{BX} = 6.8$ Hz, $J_{AB} = 16.7$ Hz, 2H), 1.21 (t, $J = 7.1$ Hz, 3H) ppm; ^{13}C NMR (125 MHz, MeOD): δ 171.3, 155.8, 134.3, 132.7, 125.0, 118.8, 112.3, 62.3, 49.8, 37.5, 14.4 ppm; HRMS (ESI) *m/z*: $[M + H]^+$ Calcd for $C_{11}H_{15}O_3NBr$ 288.0230; found 288.0233.

(S_C)-Ethyl 3-amino-2-(2-hydroxy-5-nitrophenyl) propanoate hydrochloride, **12m-(S_C)**. It was prepared following the general procedure from 470 mg of **8m-(R_S,S_C)** (1.31 mmol), and 0.5 mL of 4 N HCl/dioxane (1.96 mmol). After 24 h, it is obtained 380.5 mg of **12m-(S_C)** (1.31 mmol, quant. yield) as a brown solid; mp 175–176 °C; $[\alpha]_D^{20}$ +58.0 (*c* 1, MeOH); ^{1}H NMR (500 MHz, MeOD): δ 8.31 (d, $J = 2.7$ Hz, 1H), 8.19 (dd, $J = 2.7$ and 9.0 Hz, 1H), 7.12 (d, $J = 9.0$ Hz, 1H), 4.97 (t, $J = 6.9$ Hz, 1H), 4.15 (cd, $J = 2.6$ and 7.1 Hz, 2H), 3.20 (AB fragment of an ABX system, $\Delta\nu = 0.10$ ppm, $J_{AX} = 7.3$ Hz, $J_{BX} = 7.0$ Hz, $J_{AB} = 16.9$ Hz, 2H), 1.21 (t, $J = 7.2$ Hz, 3H) ppm; ^{13}C NMR (125 MHz, MeOD): δ 171.1, 162.5, 141.7, 127.6, 126.4, 123.8, 117.1, 62.4, 37.3, 25.7, 14.3 ppm; HRMS (ESI) *m/z*: $[M + H]^+$ Calcd for $C_{11}H_{15}O_5N_2$ 255.0975; found 255.0975.

4.2. Computational framework

Geometry optimization of the molecules was performed with Gaussian 09 [26] by using density functional theory (DFT) with B3LYP functionals and cc-pVDZ basis set [27]. Transition-state structures correspond to single imaginary frequencies. Integral equation formalism (IEF) of the polarisable continuum model (PCM) was considered for solvent effect with tetrahydrofuran as solvent [28]. Wavefunction analysis using the atoms in molecule theory was carried out as it is implemented in AIMAll software package [29]. Chemcraft software was used for the visualization of the molecules [30].

4.3. Biological studies

4.3.1. In vitro experiments

Cell Culture. All cells were cultured at 37 °C in an incubator with a humidified atmosphere containing 5% CO_2, with either Roswell Park Memorial Institute (RPMI) for N13 and 4T1, Bovine Endothelial Growth Medium (BEGM) for BAEC or (DMEM) for F98, C6, MCF7, and HeLa.

Cytotoxicity assessment. Cytotoxicity was evaluated in all cells using the MTT assay, which provides an evaluation of mitochondrial activity. The protocol is described in detail in the Supporting Information.

Co-Culture assay. N13 was first labeled with a red fluorescent dye. Then, both N13 and F98 cells were seeded in a 96-well plate. Image acquisition was performed using an Operetta High Content Screening system (PerkinElmer). Further details are given in the Supporting Information.

4.3.2. In vivo experiments

Animal experiments. Animal experiments were performed in accordance with the ethical guidelines of our local ethical committee and consistent with national regulations for the care and use of laboratory animals (R.D. 53/2013).

Tumor implantation. Tumor implantation was conducted following a previous protocol described by some of us [31]. This protocol is described in detail in the Supporting Information.

In vivo Magnetic Resonance Imaging (MRI). MRI experiments were carried out on a Bruker Biospec 9.4 T system equipped with 400 mT/m gradients, using a 20 mm-inner-diameter surface coil placed on top of the rat head for signal reception and a 72 mm volume resonator for excitation. High-resolution T_2-weighted images encompassing the entire tumor were acquired using a turbo-RARE sequence (TE = 33 ms, TR = 2500 ms, 2 averages, 384 μm in-plane resolution, and 1 mm slice thickness). 10 days after tumor implantation, coumarin derivatives were intratumorally administered at a concentration of 5 mg/kg, and their effect on tumor growth was evaluated by measuring the tumor volume using the aforementioned T_2-weighted MR images.

Author contributions

The manuscript was written through contributions of all authors. All authors have given approval to the final version of the manuscript.

Declaration of competing interest

The authors declare that they have no known competing financial interests or personal relationships that could have appeared to influence the work reported in this paper.

Data availability

Data will be made available on request.

Acknowledgment

This work was supported by the Ministerio de Ciencia, Innovación y Universidades (grant number PID2019-104767RB-I00/AEI/10.13039/501100011033), and by the Consejería de Economía, Conocimiento, Empresas y Universidad, Junta de Andalucía (grant number:US-1381590). We gratefully thank CITIUS for NMR facilities. Calculations were performed through CICA - Centro Informático Científico de Andalucía (Spain). ASC thanks funds from Junta de Andalucía (2019/FQM-106). MRI studies were performed in the ICTS "NANBIOSIS", specifically in the U28 Unit at the "Instituto de Investigación Biomédica de Málaga y Plataforma en Nanomedicina (IBIMA Plataforma BIONAND)".

Appendix A. Supplementary data

Supplementary data to this article can be found online at https://doi.org/10.1016/j.ejmech.2022.114730.

Abbreviations

BCP	bond critical point
CCP	cage critical point
GBM	glioblastoma multiforme
HMRS	High-resolution mass spectra
MRI	Magnetic Resonance Imaging
NMR	nuclear magnetic resonance spectroscopy
QTAIM	quantum theory of atoms in molecules
RCP	ring critical point
THF	tetrahydrofuran

References

[1] Y. Wang, J. Pan, R. Jiang, Y. Wang, Z. Zhou, Stereocontrolled construction of 3,4-dihydrocoumarin scaffolds with a quaternary amino acid moiety *via* chiral squaramide-catalyzed cascade michael addition/lactonization reaction, Adv. Synth. Catal. 358 (2016) 195–200, https://doi.org/10.1002/adsc.201500862.

[2] J. Modranka, A. Albercht, R. Jakibowski, H. Krawczyk, M. Rósalski, U. Krajewska, A. Janecka, A. Wyrebska, B. Rozalska, T. Janecki, Synthesis and biological evaluation of α-methylidene-δ-lactones with 3,4-dihydrocoumarin skeleton, Bioorg. Med. Chem. 20 (2012) 5017–5026, https://doi.org/10.1016/j.bmc.2012.06.022.

[3] F. Roelens, K. Huvaere, W. Dhooge, M. Van Cleemput, F. Comhaire, D. Keukeleire, Regioselective synthesis and estrogenicity of (±)-8-alkyl-5,7-dihydroxy-4-(4-hydroxyphenyl)-3,4-dihydrocoumarins, Eur. J. Med. Chem. 40 (2005) 1042–1051, https://doi.org/10.1016/j.ejmech.2005.04.010.

[4] a) K. Zhang, W. Ding, J. Sun, B. Zhang, F. Lu, R. Lai, Y. Zou, G. Yedid, Antioxidant and antitumor activities of 4-arylcoumarins and 4-aryl-3,4-dihydrocoumarins, Biochimie 107 (2014) 203–210, https://doi.org/10.1016/j.biochi.2014.03.014;
b) X.F. Zhang, H.M. Wang, Y.L. Song, L. Nie, L.F. Wang, B. Liu, P.P. Shen, Y. Liu, Isolation, structure elucidation, antioxidative and immunomodulatory properties of two novel dihydrocoumarins from, Aloe vera. Bioorg. Med. Chem. Lett. 16 (2005) 949–953, https://doi.org/10.1016/j.bmcl.2005.10.096.

[5] a) J.G. Rico, Synthesis of novel β-amino acid precursors: β-amino-hydrocoumarins as unusual aspartic acid mimetics used in fibrinogen receptor antagonists, Tetrahedron Lett. 35 (1994) 6599–6602, https://doi.org/10.1016/S0040-4039(00)73445-9;
b) J.G. Rico, R.J. Lindmark, T.E. Rogers, P.R. Bovy, A highly stereoselective michael addition to an α,β-unsaturated ester as the crucial step in the synthesis of a novel β-amino acid-containing fibrinogen receptor antagonist, J. Org. Chem. 58 (1993) 7948–7951, https://doi.org/10.1021/jo00079a054.

[6] M.D. Cordero, M. de Miguel, I. Carmona-López, P. Bonal, F. Campa, A.M. Moreno-Fernández, Oxidative stress and mitochondrial dysfunction in fibromialgia, Neuroendocrinol. Lett. 31 (2010) 169–173, https://doi.org/10.1016/j.mito.2015.01.010.

[7] a) L. Cui, D. Lv, Y. Wang, Z. Fan, Z. Li, Z. Zhou, Asymmetric formal [4 + 2] annulation of *o*-quinone methides with β-keto acylpyrazoles: a general approach to optically active trans-3,4-dihydrocoumarins, J. Org. Chem. 83 (2018) 4221–4228, https://doi.org/10.1021/acs.joc.8b00234;
b) Z.-P. Zhang, K.-X. Xie, C. Yang, M. Li, X. Li, Asymmetric synthesis of dihydrocoumarins through chiral phosphoric acid-catalyzed cycloannulation of para-quinone methides and azlactones, J. Org. Chem. 83 (2018) 364–373, https://doi.org/10.1021/acs.joc.7b02750.

[8] a) R. Devi, S.K. Das, Combining spiro-fused cyclohexadienone - tetrahydrofuran ring system with glycine: asymmetric synthesis of a new class of α-amino acid derivatives, Tetrahedron Lett. 59 (2018) 2281–2283, https://doi.org/10.1016/j.tetlet.2018.04.084;
b) B. Sun, R. Pluta, N. Kumagai, M. Shibasaki, Direct Catalytic Asymmetric Mannich-Type Reaction en Route to α-Hydroxy-β-amino Acid Derivatives, Org. Lett. 20 (2018) 526–529, https://doi.org/10.1021/acs.orglett.7b03609;
c) D.B. Chandrasekhar, S.C. Tsay, T.K. Pradhan, J.R. Hwu, Syntheses of chroman-2-ones and α-amino acids through a diastereoselective domino reaction, J. Org. Chem. 82 (2017) 5524–5537, https://doi.org/10.1021/acs.joc.7b00260.

[9] S.R. Nagarajan, B. Devadas, J.W. Malecha, H.-F. Lu, P.G. Ruminski, J.G. Tico, T. E. Rogers, L.D. Marrufo, J.T. Collins, H.P. Kleine, M.K. Lantz, J. Zhu, N.F. Green, M. A. Russell, B.H. Landis, L.M. Miller, D.M. Meyer, T.D. Duffin, V.W. Engleman, M. B. Finn, S.K. Freeman, D.W. Griggs, M.L. Williams, M.A. Nickols, J.A. Pegg, K. E. Shannon, C. Steininger, M.M. Westlin, G.A. Nickols, J.L. Keene, *R*-Isomers of Arg-Gly-Asp (RGD) mimics as potents $\alpha_V\beta_3$ inhibitors, Bioorg. Med. Chem. 15 (2007) 3783–3800, https://doi.org/10.1016/j.bmc.2007.03.034.

[10] a) M. Barczyk, S. Carrecedo, D. Gullberg, Integrins. *Cell Tissue Res.* 339 (2010) 269–280, https://doi.org/10.1007/s00441-009-0834-6;
b) G. Serini, D. Valdembri, F. Bussolino, Integrins and angiogenesis: a sticky business, Experimental Cell Res 312 (2006) 651–658, https://doi.org/10.1016/j.

yexcr.2005.10.020;
c) R.O. Hynes, The evolution of metazoan extracellular matrix, J. Cell Biol. 196 (2012) 671–679, https://doi.org/10.1083/jcb.201109041;
d) A. Van der Flier, A. Sonnenberg, Function and interactions of integrins, Cell Tissue Res. 305 (2001) 285–298, https://doi.org/10.1007/s004410100417.

[11] J. Dandriyal, R. Singla, M. Kumar, Vikas Jaitak, Recent developments of C-4 substituted coumarin derivatives as anticancer agents, Eur. J. Med. Chem. 119 (2016) 141–168, https://doi.org/10.1016/j.ejmech.2016.03.087.

[12] L. Zhang, Z. Xu, Coumarin-containing hybrids and their anticancer activities, Eur. J. Med. Chem. 181 (2016), 111587, https://doi.org/10.1016/j.ejmech.2019.111587.

[13] a) A. Chelouan, R. Recio, L.G. Borrego, E. Alvarez, N. Khiar, I. Fernandez, Sulfinamide phosphinates as chiral catalysts for the enantioselective organocatalytic reduction of imines, Org. Lett. 18 (2016) 3258–3261, https://doi.org/10.1021/acs.orglett.6b01509;
b) I. Fernandez, V. Valdivia, A. Alcudia, A. Chelouan, N. Khiar, Enantiodivergent approach to trifluoromethylated amines: a concise route to both enantiomeric analogues of calcimimetic NPS R-568, Eur. J. Org. Chem. 8 (2010) 1502–1509, https://doi.org/10.1002/ejoc.200901158;
c) I. Fernandez, V. Valdivia, N. Khiar, *N*-isopropylsulfinylimines as useful intermediates in the synthesis of chiral amines: expeditive asymmetric synthesis of the calcimimetic (+)-NPS R-568, J. Org. Chem. 73 (2008) 745–748, https://doi.org/10.1021/jo7018703.

[14] a) Z. Fei, Q. Wu, F. Zhang, Y. Cao, C. Liu, W.-C. Wen-Chung Shieh, S. Xue, J. McKenna, P. Prasad, M. Prashad, D. Baeschlin, N. Namoto, A scalable synthesis of an azabicyclooctanyl derivative, a novel DPP-4 inhibitor, J. Org. Chem. 73 (2008) 9016–9021, https://doi.org/10.1021/jo801830x;
b) G. Probst, D.L. Aubele, S. Bowers, D. Dressen, A.W. Garofalo, R.K. Hom, A. W. Konradi, J.L. Marugg, M.N. Mattson, M.L. Neitzel, C.M. Semko, H.L. Sham, J. Smith, M. Sun, A.P. Truong, X.M. Ye, Y.-Z. Xu, M.S. Dappen, J.J. Jagodzinski, P. S. Keim, B. Peterson, L.H. Latimer, D. Quincy, J. Wu, E. Goldbach, D.K. Ness, K. P. Quinn, J.-M. Sauer, K. Wong, H. Zhang, W. Zmolek, E.F. Brigham, D. Kholodenko, K. Hu, G.T. Kwong, M. Lee, A. Liao, R.N. Motter, P. Sacayon, P. Santiago, C. Willits, F. Bard, M.P. Bova, S.S. Hemphill, L. Nguyen, L. Ruslim, K. Tanaka, P. Tanaka, W. Wallace, T.A. Yednock, G.S. Basi, Discovery of (*R*)-4-Cyclopropyl-7,8-difluoro-5-(4-(trifluoromethyl)phenylsulfonyl)-4,5-dihydro-1*H*-pyrazolo[4,3-*c*]quinoline (ELND006) and (*R*)-4-Cyclopropyl-8-fluoro-5-(6-(trifluoromethyl)pyridin-3-ylsulfonyl)-4,5-dihydro-2*H*-pyrazolo[4,3-*c*]quinoline (ELND007): metabolically stable γ-secretase inhibitors that selectively inhibit the production of amyloid-β over notch, J. Med. Chem. 56 (2013) 5261–5274, https://doi.org/10.1021/jm301741t;
c) A.W. Patterson, W.J.L. Wood, M. Hornsby, S. Lesley, G. Spraggon, J.A. Ellman, Identification of selective, nonpeptidic nitrile inhibitors of cathepsin S using the substrate activity screening method, J. Med. Chem. 49 (2006) 6298–6307, https://doi.org/10.1021/jm060701s;
d) M.T. Robak, M.A. Herbage, J.A. Ellman, Synthesis and applications of *tert*-butanesulfinamide, Chem. Rev. 119 (1997) 9913–9914, https://doi.org/10.1021/cr900382t;
e) A. Chelouan, R. Recio, L.G. Borrego, E. Alvarez, N. Khiar, I. Fernandez, Sulfinamide phosphinates as chiral catalysts for the enantioselective organocatalytic reduction of imines, Org. Lett. 18 (2016) 3258–3261, https://doi.org/10.1021/acs.orglett.6b01509;
f) L.G. Borrego, R. Recio, E. Álvarez, A. Sánchez-Coronilla, N. Khiar, I. Fernández, Steric tuning of sulfinamide/sulfoxides as chiral ligands with C_1, pseudo-*meso*, and pseudo-C_2 symmetries: application in rhodium(I)-Mediated arylation, Org. Lett. 21 (2019) 6513–6518, https://doi.org/10.1021/acs.orglett.9b02405.

[15] a) D.A. Cogan, G. Liu, J. Ellman, Asymmetric synthesis of chiral amines by highly diastereoselective 1,2-additions of organometallic reagents to N-tert-Butanesulfinyl imines, Tetrahedron 55 (1999) 8883–8904, https://doi.org/10.1016/S0040-4020(99)00451-2;
b) D.A. Pflum, D. Krishnamurthy, Z. Han, S.A. Wald, C.H. Senanayake, Asymmetric synthesis of cetirizine dihydrochloride, Tetrahedron Lett. 43 (2002) 923–926, https://doi.org/10.1016/S0040-4039(01)02294-8;
c) N. Plobeck, D. Powell, Asymmetric synthesis of diarylmethylamines by diastereoselective addition of organometallic reagents to chiral N-tert-butanesulfinimines: switchover of diastereofacial selectivity, Tetrahedron: Asymmetry 13 (2002) 303–310, https://doi.org/10.1016/S0957-4166(02)00099-X.

[16] T.P. Tang, J.A. Ellman, The *tert*-butanesulfinyl group: an ideal chiral directing group and boc-surrogate for the asymmetric synthesis and applications of β-amino acids, J. Org. Chem. 64 (1999) 12–13, https://doi.org/10.1021/jo9820824.

[17] Y. Li, D. Li, T. Zheng, H. Li, X. Ren, Double-addition reaction of aryl methyl sulfones with N-tert-Butylsulfinyl imines: diastereoselective and concise synthesis of 2-sulfonylated 1,3-diamines, Chem. Eur J. 20 (2014) 14986–14990, https://doi.org/10.1002/chem.201404009.

[18] a) R.F. Bader, Atoms in Molecules – A Quantum Theory, Oxford University Press, 1990;
b) C.F. Matta, R.J. Boyd, The Quantum Theory of Atoms in Molecules: from Solid State to DNA and Drug Design, Wiley-VCH, Weinheim, 2007.

[19] a) C. Carraro, A. Francke, A. Sosic, F. Kohl, T. Helbing, M. de Franco, D. Fabris, R. Göttlich, B. Gatto, Behind the mirror: chirality tunes the reactivity and cytotoxicity of chloropiperidines as potential anticancer agents, ACS Med. Chem. Lett. 10 (2019) 552–557, https://doi.org/10.1021/acsmedchemlett.8b00580;
b) E. Rodríguez-Arce, P. Cancino, M. Arias-Calderón, P. Silva-Matus, M. Saldías, Oxoisoaporphines and aporphines: versatile molecules with anticancer effects, Molecules 25 (2020) 108, https://doi.org/10.3390/molecules25010108.

[20] S. Daubeuf, C. Bordier, D. Hudrisier, E. Joly, Suitability of various membrane lipophilic probes for the detection of trogocytosis by flow cytometry, Cytometry 75A (2009) 380–389, https://doi.org/10.1002/cyto.a.20679.

[21] a) J. Drogosz-Stachowicz, A. Długosz-Pokorska, K. Gach-Janczaka, A. Jaskulsk, J. Tomasz, A. Janecka, Molecular mechanisms of apoptosis induced by a novel synthetic quinolinone derivative in HL-60 human leukemia cells, Chem. Biol. Interact. 320 (2020), 109005, https://doi.org/10.1016/j.cbi.2020.109005;
b) A. Tabll, H. Ismail, The use of flow cytometric DNA ploidy analysis of liver biopsies in liver cirrhosis and hepatocellular carcinoma: from liver biopsy, Intech (2011), https://doi.org/10.5772/19384.

[22] W. Wang, H.Y. Cho, R. Rosenstein-Sisson, N.I. Marín-Ramos, R. Price, K. Hurth, A. H. Schönthal, F.M. Hofman, T.C. Chen, Intratumoral delivery of bortezomib: impact on survival in an intracranial glioma tumor model, J. Neurosurg. 128 (2018) 695–700, https://doi.org/10.3171/2016.11.JNS161212.

[23] J.A. Fernandez-Salas, M.M. Rodriguez-Fernandez, M.C. Maestro, J.L. Garcia-Ruano, Synthesis of enantiomerically pure (α-Phenylalkyl)amines with susbstituents at the ortho position through diastereo-selective radical alkylation reaction of sulfinylimines, Eur. J. Org. Chem. 2014 (2014) 5265–5272, https://doi.org/10.1002/ejoc.201402355.

[24] M.S. Maji, R. Fröhlich, A. Studer, Desymmetrization of metallated cyclohexadienes with chiral *N-tert*-butylsufinyl imines, Org. Lett. 10 (2008) 1847–1850, https://doi.org/10.1021/ol800478q.

[25] Y.-Y. Shen, Y. Li, B. Wang, X. Li, Anion binding by *tert*-butanesulfinamide based phenol reactions, Tetrahedron Lett. 57 (2016) 582–586, https://doi.org/10.1016/j.tetlet.2015.12.090.

[26] M.J. Frisch, G.W. Trucks, H.B. Schlegel, G.E. Scuseria, M.A. Robb, J.R. Cheeseman, G. Scalmani, V. Barone, B. Mennucci, G.A. Petersson, H. Nakatsuji, M. Caricato, X. Li, H.P. Hratchian, A.F. Izmaylov, J. Bloino, G. Zheng, J.L. Sonnenberg, M. Hada, M. Ehara, K. Toyota, R. Fukuda, J. Hasegawa, M. Ishida, T. Nakajima, Y. Honda, O. Kitao, H. Nakai, T. Vreven, J.A. Montgomery Jr., J.E. Peralta, F. Ogliaro, M. J. Bearpark, J. Heyd, E.N. Brothers, K.N. Kudin, V.N. Staroverov, R. Kobayashi, J. Normand, K. Raghavachari, A.P. Rendell, J.C. Burant, S.S. Iyengar, J. Tomasi, M. Cossi, N. Rega, N.J. Millam, M. Klene, J.E. Knox, J.B. Cross, V. Bakken, C. Adamo, J. Jaramillo, R. Gomperts, R.E. Stratmann, O. Yazyev, A.J. Austin, R. Cammi, C. Pomelli, J.W. Ochterski, R.L. Martin, K. Morokuma, V.G. Zakrzewski, G.A. Voth, P. Salvador, J.J. Dannenberg, S. Dapprich, A.D. Daniels, Ö. Farkas, J. B. Foresman, J.V. Ortiz, J. Cioslowski, D.J. Fox, Gaussian 09, Gaussian, Inc., Wallingford, CT, USA, 2009.

[27] a) C.T. Lee, W.T. Yang, R.G. Parr, Development of the colle-salvetti correlation-energy formula into a functional of the electron-density, Phys. Rev. B 37 (2) (1988) 785–789, https://doi.org/10.1103/PhysRevB.37.785;
b) A.D. Becke, Density-functional thermochemistry. III. The role of exact exchange, J. Chem. Phys. 98 (1993) 5648–5652, https://doi.org/10.1063/1.464913;
c) T.H. Dunning, Gaussian-basis sets for use in correlated molecular calculations .1. The atoms boron through neon and hydrogen, J. Chem. Phys. 90 (2) (1989) 1007–1023, https://doi.org/10.1063/1.456153.

[28] a) E. Cances, B. Mennucci, J. Tomasi, A new integral equation formalism for the polarizable continuum model: theoretical background and applications to isotropic and anisotropic dielectrics, J. Chem. Phys. 107 (8) (1997) 3032–3041, https://doi.org/10.1063/1.474659;
b) B. Mennucci, E. Cances, J. Tomasi, Evaluation of solvent effects in isotropic and anisotropic dielectrics and in ionic solutions with a unified integral equation method: theoretical bases, computational implementation, and numerical applications, J. Phys. Chem. B 101 (49) (1997) 10506–10517, https://doi.org/10.1021/jp971959k.

[29] T.A.K. Gristmill, *AIMAll (Version 11.08.23)* Todd A. Keith Gristmill Software, aim.tkgristmill.com), Overland Park KS, USA, 2011.

[30] www.chemcraftprog.com.

[31] S. Lope-Piedrafita, M.L. Garcia-Martin, J.P. Galons, R.J. Gillies, T.P. Trouard, Longitudinal diffusion tensor imaging in a rat brain glioma model, NMR Biomed. 21 (2008) 799–808, https://doi.org/10.1002/nbm.1256.